

Executive Summary

On August 30, 1999, the South Florida Water Management District (District) contracted with DB Environmental, Inc. (DBE) to perform a 100-week evaluation of Submerged Aquatic Vegetation/Limerock (SAV/LR) Treatment System technology for reducing phosphorus (P) discharge from Everglades Agricultural Area (EAA) waters. The objectives of this project are to assess the long-term, sustainable performance of this technology, and to develop design and operational criteria for a full-scale SAV/LR system. For this effort, we are performing scientific and engineering work at Stormwater Treatment Area (STA)-1W at several spatial scales: outdoor microcosms and mesocosms, test cells (0.2 ha), Cell 4 (146 ha) and Cell 5 (1,100 ha). This document is a quarterly progress report describing work efforts of DBEL's project team from November 2000 – January 2001. Key accomplishments and findings are as follows.

During this quarter, we continued using existing mesocosms and test cells at both the North and South Advanced Treatment Technology (NATT and SATT) sites of STA-1W to assess effects of hydraulic loading rates, water type (Post-BMP vs. Post-STA), and system configuration on SAV/LR phosphorus removal performance. We also performed water column sampling in Cell 4 to characterize internal P concentration gradients, initiated a mesocosm drydown (SRP release) study, and characterized particles in the inflow and outflow of Cell 4, and of two test cells.

We continued operation of a long-term, flow-through microcosm study to assess the effects of soluble reactive P, calcium and alkalinity on P removal performance. SAV performance is being tested at high and low Ca (80 - 100 vs. ~20 - 30 mg/L) and alkalinity (325 - 375 vs. ~75 - 150 mg CaCO₃/L) concentrations, as well as high (125 - 160 µg/L) and low (20 - 40 µg/L) SRP concentrations. Eight microcosms containing *Najas guadalupensis* are receiving the various Ca/alkalinity and SRP media at a hydraulic loading rate of 9.6 cm/day (3.5 day hydraulic retention time). To date, SAV cultured under the high Ca/alkalinity regimes has provided lower outflow TP concentrations than under the low Ca/alkalinity concentrations. For example, for the “low SRP” microcosms, outflow TP concentrations have averaged 12 and 17 µg/L under high and low Ca/alk. conditions, respectively. Under “high SRP” conditions, outflow TP concentrations have averaged 26 µg/L (high Ca/alk.) and 64 µg/L (low Ca/alk.).

We completed operation of a pulse loading study, using SAV mesocosms that previously had received hydraulic loading rates (HLRs) of 11, 22 and 53 cm/day. Our hydraulic loading schedule for the mesocosms was similar to the “STA-2” hydraulic loading data set in the following respects: our protocol had the same average seasonal flow patterns; the same percentage of “no-flow” weeks; and, the same standard deviation on a seasonal basis. We scaled (increased) the STA-2 HLRs by factors of 5X, 10X and 25X, with flow provided to the mesocosms in two-week long pulses. These increased flows were selected to match the prior, high HLRs (11 – 53 cm/day) to the SAV mesocosms, thus providing continuity with previous HLR studies.

This study revealed that low pulse-loading regime provided about the same outflow TP concentrations (25 µg/L) as those that receive a low, steady state loading (21 µg/L). However, the moderately and highly loaded pulsed systems produced substantially higher outflow TP concentrations than mesocosms operated under steady state conditions (51 vs. 38 µg/L at high load; 31 vs. 20 µg/L at moderate load). These data suggest that pulse-loading effects would be dramatic at the inflow region of a SAV-based STA cell, but would gradually be “dampened out” with passage through the wetland.

Upon completion of the pulse-loading study, we initiated a “drydown” study to assess export of P from dessicated sediments and vegetation following drydown and reflooding. Two mesocosms, one that previously received a high hydraulic loading (53 cm/day) of Post-BMP waters, and one that received a low hydraulic loading (11 cm/day), are being used for the study. As a subset of this experiment, we also are assessing the export of sediment P as a function of dessication time (= moisture content).

To compare relative performance of SAV and cattail-dominated wetlands, we continued monitoring of shallow mesocosms containing these respective vegetative communities. The SAV mesocosms continued to outperform cattail mesocosms operated at similar depths (0.4m) and HLRs (10 cm/day). For the quarter we observed a 60% reduction in TP concentration (from

40 to 16 µg/L) in the SAV-dominated mesocosms, while only a 32% decrease in TP concentration (from 43 to 29 µg/L) was observed for the cattail mesocosms.

In order to assess performance of a SAV/periphyton system under increased flow velocities, we modified the three shallow (0.09 m deep) SAV/periphyton/LR raceways to receive Post-STA waters in a sequential, rather than parallel fashion. The flow path is now tripled, and the HLR has been increased to 66 cm/day, providing a velocity (0.36 cm/sec.) comparable to that of full-scale STA cells. Phosphorus removal performance of this system will be assessed for a six-month period.

We continued monitoring the 0.4 m deep tanks at the SATT site that contain SAV cultured on muck, sand and limerock substrates. During the quarter, inflow TP concentrations to these mesocosms averaged 19 µg/L and outflow TP concentrations from all three substrate treatments were in the range of 9 – 11 µg/L.

During this quarter we completed a small-scale filtration study at the SATT site, designed to test the effectiveness of various filter media as a “back-end” particle filtration step for SAV wetlands. Filter media that were evaluated included: coarse (3.4 – 6.9 mm), medium (2.0 – 3.4mm) and fine (0.25 – 0.85 mm) quartz pebbles/sand; coarse and medium sized limerock; coarse and medium sized Ca/Mg silicate materials (Pro-Sil Plus™); and a fine, iron-coated quartz sand. These materials encompass filter media that are inert, and therefore should only provide particulate filtration, as well as those with chemical characteristics (high calcium or iron content) that should further contribute to soluble P removal.

During the fourteen week (August 18 – November 17, 2000) study, coarse and medium sizes of limerock and Pro-Sil Plus™ were found to be the most effective filter media, reducing TP concentrations from a mean of 17 µg/L to 13-14 µg/L. We could not distinguish any differences in P removal among the three grain sizes (fine, medium, coarse) of quartz sand: column effluents averaged 14-17 µg/L compared to 17 µg/L for the inflow. The iron-coated sand was the least effective filter media, providing an export of TP for the duration of the study. For all

media, most of the P removal could be attributed to the filtering of particulate P; there were negligible reductions in SRP and total soluble P among all media types and sizes.

We are now completing a study in which particles from inflow and outflow waters of Cell 4 and two north test cells (one SAV, one cattail) were isolated and characterized. Different size fractions of particles were concentrated into slurries with a tangential flow filtration device. The isolated particles were characterized with respect to size, surface charge, mineralogical analysis and chemical analyses. While our data analyses are still underway, our initial characterization demonstrates that particles from the inflow and outflow of all systems consist of calcite, silicate and organic matter. Calcite levels were found to be highest in the outflow waters from Cell 4.

On December 19, 2000, we performed our third intensive water quality sampling within Cell 4. This sampling was performed during a period of high inflow TP concentrations (109 ug/L), as well as pronounced bird activity. Additional sampling events in Cell 4 will be conducted during 2001.

The four 0.2 ha SAV test cells are being operated at HLRs of 11 cm/day (north cells) and 5 cm/day (south cells). The north test cell inflow TP concentrations during the quarter averaged only 39 µg/L. Outflow concentrations from both NTC-1 and NTC-15 dropped to as low as 10 µg/L during the quarter. As has been observed previously, the two south test cells continue to provide different levels of performance. STC-9, which is an SAV wetland equipped with a limerock berm, reduced average inflow TP levels of 17 to 14 µg/L. STC-4, an SAV wetland without a limerock berm, provided a slight export of TP during the quarter.

In November 2000, we evaluated SAV colonization at the 120 monitoring stations that we had established in STA-1W Cell 5 during February 2000. Submerged vegetation, in particular *Najas* and *Ceratophyllum*, are continuing to expand throughout the wetland. The aggressive aquatic weed, *Hydrilla verticillata*, also is beginning to expand its coverage in Cell 5. Regions of this wetland with moderate to dense SAV biomass exhibited lower water column SRP levels than regions with little or no SAV coverage.

Table of Contents

Introduction	1
Project Team Members.....	1
Task 5. Mesocosm Investigations	2
Effects of Calcium/Alkalinity and Soluble Reactive Phosphorus Concentrations on Phosphorus Coprecipitation (Subtask 5i)	2
Long-Term Monitoring of P Removal Performance by SAV Mesocosms (Subtask 5iv).....	12
Effects of Pulse Loading on Phosphorus Removal Performance by SAV Communities (Subtask 5v).....	14
Effects of Dryout and Reflooding on Phosphorus Retention (Subtask 5v).....	19
Comparison of Phosphorus Removal Performance by Cattail- and SAV-Dominated Systems (Subtask vi)	21
Shallow Low Velocity SAV/Periphyton/Limerock Systems (Subtask 5vii).....	22
Effects of Flow Velocity on Phosphorus Removal by Shallow SAV/Periphyton Communities (Subtask 5viii)	22
Growth of SAV in Post-STA Waters on Muck, Limerock and Sand Substrates (Subtask 5ix).....	26
Effects of Filter Media Size and Type on P Removal Performance (Subtask 5x)	29
Particulate Phosphorus and Dissolved Organic Phosphorus Characterization and Stability (Subtask 5xi)	37
Particulate Phosphorus Characterization in the Inflows and Outflows of Test Cells and Cell 4.....	37
References	50
Task 6. Test Cell Investigations	52
Task 9. Cell 4 Performance Monitoring.....	55
References	55
Task 10. Cell 5 SAV Inoculation and Monitoring	56

List of Figures

Figure 1.	Flow chart detailing the experimental design for the flow-through Coprecipitation Experiment.	4
Figure 2.	The total soluble P concentrations in the inflows and outflows of culture tanks containing <i>Najas</i> exposed to low and high calcium and alkalinity treated culture media with and without added soluble reactive P.....	8
Figure 3.	The pH values of the inflows and outflows of high and low calcium and alkalinity treated culture media with and without added soluble reactive P (SRP).....	9
Figure 4.	Total alkalinity concentrations in the inflows and outflows of culture tanks containing <i>Najas</i> exposed to SRP amended and unamended culture media under high and low calcium and alkalinity concentrations.....	10
Figure 5.	Dissolved calcium concentrations in the inflows and outflows of culture tanks containing <i>Najas</i> exposed to SRP amended and unamended culture media under high and low calcium and alkalinity concentrations.....	11
Figure 6.	Mean soluble reactive, particulate, and dissolved organic phosphorus concentrations in the inflow and outflow from SAV mesocosms and outflow from subsequent limerock filters.	13
Figure 7.	Mean outflow total P concentrations in duplicate pulse loaded mesocosms compared to a constant load mesocosm operated at a similar average hydraulic loading rate of 11 cm/day.....	16
Figure 8.	Mean outflow total P concentrations in duplicate pulse loaded mesocosms compared to a constant loaded mesocosm operated at a similar average hydraulic loading rate of 23 cm/day.....	17
Figure 9.	Mean outflow total P concentrations in duplicate pulse loaded mesocosms compared to a constant loaded mesocosm operated at a similar average hydraulic loading rate of 53 cm/day.....	18
Figure 10.	Mean total phosphorus concentrations in the inflows and outflows from SAV- and cattail-dominated mesocosms operated since December 1998.	23
Figure 11.	Mean soluble reactive, particulate and dissolved organic phosphorus concentrations in the inflows and outflows from SAV- and cattail-dominated mesocosms during the November 2000-January 2001 quarter.	24
Figure 12.	Total phosphorus concentrations in the inflow and outflows of triplicate shallow, low velocity, SAV/periphyton raceways and in the outflow of the subsequent limerock beds.....	25
Figure 13.	Sampling locations for the experiment on the effects of flow velocity on P removal by a shallow SAV/periphyton community.	26
Figure 14.	Total P concentrations in the inflow and outflow of a shallow raceway dominated by a mixed <i>Chara</i> /periphyton community and in the outflow of a subsequent limerock bed at a hydraulic loading rate of 66 cm/day	27

Figure 15.	Mean total phosphorus concentrations in the inflow and outflows of duplicate SAV treatment trains operated on sand, limerock and muck substrates from July 1999 to March 2001.....	28
Figure 16.	Mean (\pm s.d.) total phosphorus concentrations in the inflow and outflow of duplicate filter columns with each pair containing one of three size fractions of quartz “sand”	31
Figure 17.	Mean total phosphorus concentration in the inflow and outflows of duplicate filter columns with each pair containing one of two size fractions of limerock..	32
Figure 18.	Mean total phosphorus concentration in the inflow and outflows of duplicate filter columns with each pair containing one of two size fractions of Pro-Sil® (Ca-Mg silicate).....	33
Figure 19.	Mean total phosphorus concentrations in the inflow and outflows of duplicate filter columns with each pair containing a coarse grade of one of three substrate types..	34
Figure 20.	Mean total phosphorus concentrations in the inflow and outflows of duplicate filter columns with each pair containing a medium grade of one of three substrate types.	35
Figure 21.	Mean (\pm s.d.) soluble reactive phosphorus concentrations in the inflow and outflow of duplicate iron-coated sand filter columns.....	36
Figure 22.	X-ray diffraction (XRD) patterns of TFF-concentrated particulates from Cell 4 and test cells.....	44
Figure 23.	Thermal gravimetric weight loss curves for particulates collected from Cell 4 outflow (top) and inflow region (bottom), shown as examples.	45
Figure 24.	Algal abundance illustrated in four-image composite of SEM micrographs (clockwise from upper left) a) centric diatoms present in suspended solids from Cell 2 outflow in the September sample magnified 500x; b) diatoms from “a)” magnified 2700x; c) C-based algal ‘cells’ from Cell 2 outflow in the August sample; d) C- based cells and both centric and pinnate diatoms present in Cell 4 inflow region during September.....	46
Figure 25.	Two six-image composites of SEM micrographs. a) Left composite: At upper left is the same secondary electron image shown in Figure 24b. Other images are elemental dot maps of Fe, Si, P, S, and Ca, showing an association of Si and P with diatoms. b) Right composite: At upper left is a higher magnification image of the largest diatom shown in the right composite.....	47
Figure 26.	Scatter plots of particulate P with particulate organic matter and suspended solids.	48
Figure 27.	Scatter plots of particulate P with particulate CaCO ₃ and particulate organic matter.	49
Figure 28.	Total phosphorus concentrations in the inflows and outflows from north test cells NTC-1 and NTC-15.	53

Figure 29.	Total phosphorus concentrations in the inflows and outflows from south test cells STC-4 and STC-9.....	54
Figure 30.	Cell 5 SAV Colonization: Presence and distribution of <i>Najas</i> beds during four 120-station visual surveys.	57
Figure 31.	Cell 5 SAV Colonization: Presence and distribution of <i>Ceratophyllum</i> beds during four 120-station visual surveys.	58
Figure 32.	Cell 5 SAV Colonization: Presence and distribution of <i>Hydrilla</i> beds during two 120-station visual surveys.	59
Figure 33.	Relationship between SAV biomass and water column SRP concentration at 24 stations internal to Cell 5 on two sampling dates, August 24 and November 30, 2000.....	60
Figure 34.	Total phosphorus and apparent color concentrations in the outflow region (inset) of Cell 5.	61

List of Tables

Table 1.	Final concentration of nutrients and micronutrients amended to W. Palm Beach tap water.....	5
Table 2.	Mean (\pm 1 s.d.) total P, TSP, SRP, dissolved Ca and alkalinity concentrations in the inflows and outflows from duplicate aquaria operated under four treatments during the November - January quarter.	6
Table 3.	Total phosphorus concentrations ($\mu\text{g/L}$) in the inflows, SAV outflows and limerock (LR) outflows of mesocosms operated at hydraulic retention times (HRT) of 1.5, 3.5 and 7.0 days since June 1998.	12
Table 4.	Forty-week (Feb. 20 - Nov. 24, 2000) pulse loading schedule for low, medium, and high loaded mesocosms.....	14
Table 5.	Average total phosphorus concentrations in the water column (outflow region) of NATT site pulse loaded mesocosms, during quiescent (7 two-week periods) and flowing (13 two-week periods) conditions.	15
Table 6.	Chemical characteristics of the inflows and outflows of mesocosms receiving high (53 cm/day) and low (11 cm/day) HLRs, and of outflows from downstream limerock barrels, during a six week baseline monitoring period prior to dry-down.	19
Table 7.	Characteristics of incubation overlying water collected from Cell 4 Inflow on January 10, 2001.....	20
Table 8.	Mean (\pm 1 s.d.) total phosphorus concentrations in the inflow and outflows from SATT mesocosms established on muck, limerock and sand substrates during the two most recent quarters.	29
Table 9.	Mean (\pm 1 s.d.) TP, SRP, PP, DOP, calcium and alkalinity concentrations in the inflow and outflows of filter media columns during the August 18-November 17, 2000 period of record.	30

Introduction

On August 30, 1999, the District contracted with DB Environmental, Inc. (DBE) to design, construct, operate, and evaluate a 100-week, multi-scale demonstration of SAV/Limerock Treatment System technology for reducing phosphorus (P) discharge from Everglades Agricultural Area (EAA) waters. The objectives of this project are to:

- Design and execute a scientific and engineering research plan for further evaluation of the technical, economic and environmental feasibility of using SAV/LR system for P removal at both the basin and sub-basin scale.
- Obtain samples adequate to conduct a Supplemental Technology Standard of Comparison (STSOC) analysis.
- Provide information and experience needed to design a full-scale SAV/LR system.

This document is a progress report for the fifth quarter describing work efforts during November 2000 – January 2001. This report focuses on methodology and findings from the mesocosm experiments (Task 5), test cell studies (Task 6), Cell 4 performance monitoring (Task 9), and Cell 5 inoculation studies (Task 10).

Project Team Members

DB Environmental, Inc. (DBE) is being assisted in this research and demonstration effort by several groups of engineers and scientists. The engineering firm Milian, Swain and Associates from Miami, FL, is providing technical field support for this project. The scientific and engineering firm HSA/Conestoga Rovers and Associates (West Palm Beach, FL) is providing engineering design and field assistance with several filtration components of this study. Particle analyses and assessments of dissolved organic P stability are being performed by the Soil and Water Science Department of the University of Florida, Gainesville, FL. Engineering issues pertaining to full-scale SAV wetlands are being addressed by Wetland Studies and Solutions, Inc., of Chantilly, VA.

Task 5. Mesocosm Investigations

During November 2000 - January 2001, we continued using existing mesocosms at both the North and South Advanced Treatment Technology sites of STA-1W to assess effects of hydraulic loading rates, water type (Post-BMP vs. Post-STA), and system configuration on P removal performance. Several new experiments (e.g. flow-through coprecipitation studies (5i)) were initiated during the quarter, while others were concluded (e.g. pulse loading (5v)). Activities are listed below by experimental subtask.

Effects of Calcium/Alkalinity and Soluble Reactive Phosphorus Concentrations on Phosphorus Coprecipitation (Subtask 5i)

Findings from our Phase I research using Post-BMP waters suggest that P removal in an SAV system is controlled in part by water column hardness and alkalinity. The first experiment performed in April 2000, entailed subjecting previously conditioned P-“enriched” and P-“deficient” *Najas* to a constant SRP concentration at high and low levels of calcium and alkalinity over a two-day measurement period. The relative importance of P uptake by SAV vs. coprecipitation of P in the water column was evaluated. The nutritional status of *Najas* tissues was the dominant factor influencing SRP removal rate differences between treatments.

Our second experiment began in November 2000. Factors not explored in the short-term experiment, such as the effects of SRP concentrations on the rate and extent of P coprecipitation, are being pursued in this experiment where a longer incubation period (3 months), using flow-through systems, is being utilized.

Tap water from the City of West Palm Beach was selected as the experimental source water because of its consistently low Ca (30 mg/L) and alkalinity (56 mg CaCO₃/L) concentrations relative to the 71 mg Ca/L and 227 mg CaCO₃/L alkalinity measured in Post-BMP agricultural drainage waters (ADW). We chose to add salts to the tap water to reach the desired alkalinity (375 mg CaCO₃/L) and Ca (100 mg Ca/L) concentrations rather than attempt to chemically remove them from the Post-BMP ADW. Opting for chemical removal would alter the water chemistry to such a degree that it would invalidate any comparison between low Ca/alkalinity (chemically “softened”) and untreated high Ca/alkalinity waters.

Because the West Palm Beach tap water has a chlorine residual and varying concentrations of SRP, dechlorination and SRP stripping were found to be necessary pre-treatment steps. This was accomplished by placing water hyacinths (*Eichhornia crassipes*) in the tap water reservoir for seven days. After the seven-day contact with water hyacinths, the water was pumped in 151L batches to four 208-liter holding reservoirs (Figure 1). The following Ca, alkalinity, and SRP amendments were added to each of the reservoirs:

1. Treatment #1 – Low calcium/alkalinity (unamended) and low SRP (stripped with water hyacinth beforehand)
2. Treatment #2 – Low calcium/alkalinity (unamended) and high SRP (stripped, then amended with 125 µg SRP/L)
3. Treatment #3 – High calcium/alkalinity (amended to a final concentration of 100 mg Ca/L and 375 mg CaCO₃ /L) and low SRP (stripped)
4. Treatment #4 - High calcium/alkalinity (amended to a final concentration of 100 mg Ca/L and 375 mg CaCO₃ /L) and high SRP (stripped, then amended with 125 µg SRP/L)

In addition to the Ca, alkalinity, and SRP amendments, all the barrels received inorganic N, potassium, and micronutrient supplements (Table 1). After adding the nutrient amendments, the content of each barrel was pumped to duplicate 75-liter microcosms (Figure 1). Each of the eight microcosms (duplicates x 4 treatments) was initially stocked with 800 g (fresh wt) of *Najas guadalupensis*. No sediment was added to the microcosms.

A flow rate of 12 mL/min (17.3 L/day) was provided to each of the microcosms, which contained 60.6 L (16 gal) of water. This produced a HRT of 3.5 days (HLR=9.6 cm/day).

Composites of three grabs per week were collected at each sampling location (Figure 1) for TP, SRP, TSP, Ca, alkalinity, and conductance measurements. In addition to the composite sampling, we also collected grab samples after each time a new batch of source water was

amended and stored within the holding tanks (Figure 1). Water temperature and pH measurements were taken in the field for each.

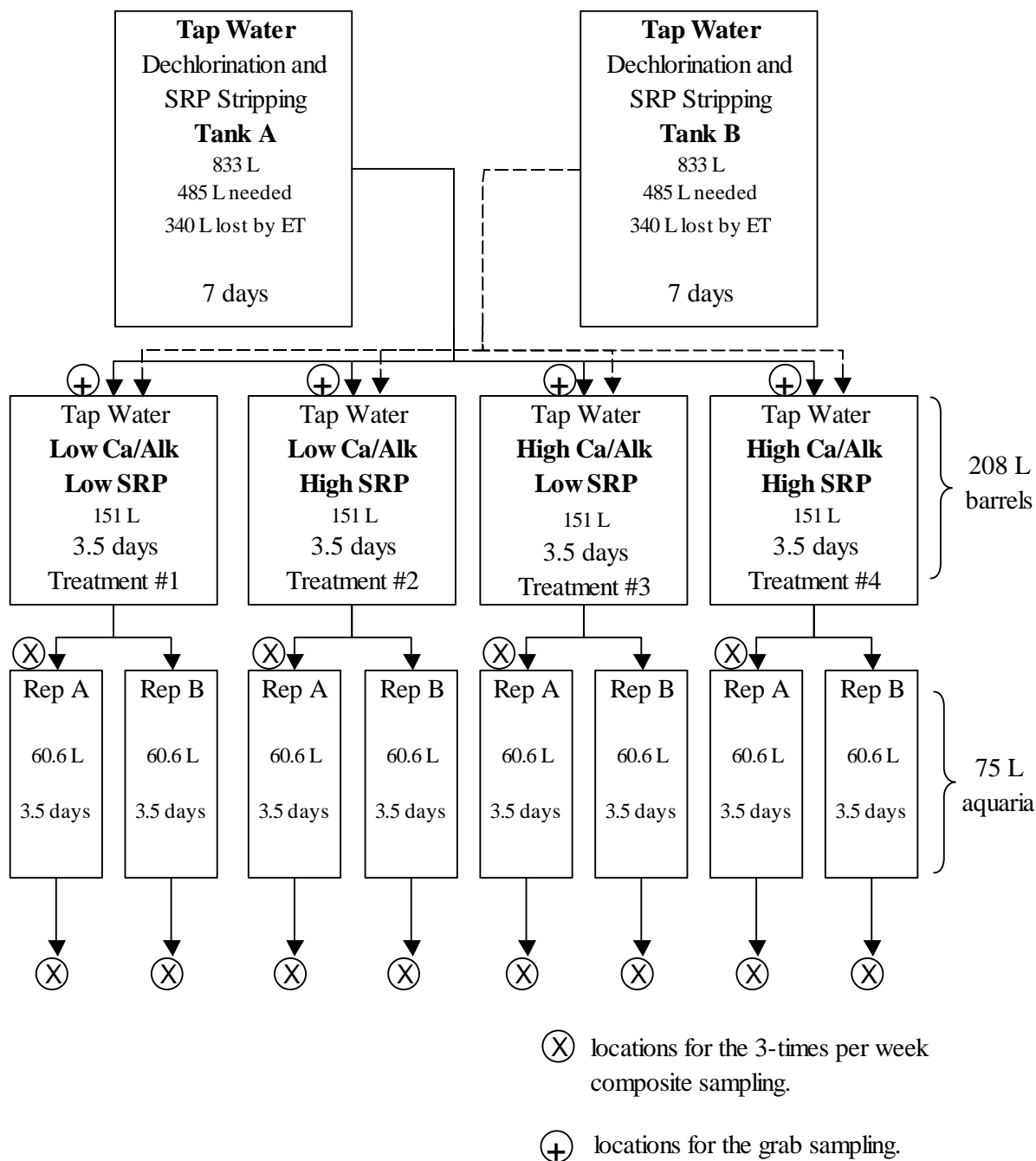


Figure 1. Flow chart detailing the experimental design for the flow-through Coprecipitation Experiment.

Table 1. Final concentration of nutrients and micronutrients amended to W. Palm Beach tap water.

Compound	Nutrient	Final Concentration
KCl	K ⁺	10.8 mg/L *
NH ₄ Cl	NH ₄ ⁺	0.5 mg N/L
KNO ₃	NO ₃ ⁻	0.5 mg N/L
H ₃ BO ₃	B	10.8 µg/L
MnSO ₄ ·H ₂ O	Mn	10.8 µg/L
ZnSO ₄ ·7H ₂ O	Zn	5.2 µg/L
CuSO ₄ ·5H ₂ O	Cu	1.2 µg/L
(NH ₄) ₆ Mo ₇ O ₂₄ ·7H ₂ O	Mo	0.4 µg/L
FeCl ₃ ·6H ₂ O	Fe (in EDTA)	16 µg/L
Na ₂ EDTA	EDTA	94 µg/L
Cyanocobalamin	B-12	3 µg/L

* 9.4 mg/L from KCl and 1.4 mg/L from KNO₃

During the first three months of operation, inflow amendments for each treatment were re-adjusted to represent calcium and alkalinity concentrations more typical for levels measured in post-BMP waters. Beginning November 22 the phosphorus amendment was increased from 125 to 160 µg/L. The Ca/alk amendments were reduced from target concentrations of 100 to 80 mg Ca/L and from 375 to 325 mg CaCO₃/L on January 26, 2001.

During the November–January quarter, mean inflow TSP concentrations were comparable between P-amended treatments (#2 and #4 in Table 2) and between unamended treatments (#1 and #3). Calcium and alkalinity concentrations were also comparable between like treatments, as shown in Table 2. Outflow calcium and alkalinity concentrations were similar for both the high and low SRP concentrations in the high Ca/alk treatments, suggesting that at the experimental concentrations of 34 - 171 µg TP/L, P concentration had no effect on calcium or alkalinity removals.

Table 2. Mean (± 1 s.d.) total P, TSP, SRP, dissolved Ca and alkalinity concentrations in the inflows and outflows from duplicate aquaria operated under four treatments during the November - January quarter.

	Treatment #1 Low Ca/alk Low P	Treatment #2 Low Ca/alk High P	Treatment #3 High Ca/alk Low P	Treatment #4 High Ca/alk High P
TP ($\mu\text{g/L}$)				
Inflow	38	166	34	171
Outflow	17 ± 3	64 ± 7	12 ± 2	26 ± 3
<i>TP Removal</i>	21	102	22	145
TSP ($\mu\text{g/L}$)				
Inflow	27	157	26	163
Outflow	9 ± 1	51 ± 6	7 ± 2	17 ± 3
<i>TSP Removal</i>	18	106	19	146
SRP ($\mu\text{g/L}$)				
Inflow	17	142	13	113
Outflow	2 ± 0	36 ± 7	2 ± 1	7 ± 2
<i>SRP Removal</i>	15	106	11	106
Alkalinity ($\text{mg CaCO}_3/\text{L}$)				
Inflow	63	62	340	339
Outflow	69 ± 3	72 ± 2	270 ± 10	266 ± 7
<i>Alkalinity Removal</i>	-6	-10	70	73
Diss. Calcium (mg/L)				
Inflow	26	26	85	84
Outflow	28 ± 1	29 ± 1	57 ± 3	56 ± 2
<i>Calcium Removal</i>	-2	-3	28	28

Considering that both SRP and dissolved organic carbon (and thus dissolved organic P [DOP]) can both be coprecipitated with CaCO_3 (Seuss 1970; Murphy et al. 1983; Danen-Louwerse et al. 1995), we examined the TSP component of our analytical data for the relevance of the P coprecipitation process. For these first three months of the experiment, TSP was reduced to a greater extent in the high Ca/alk-high SRP treatment than in the low Ca/alk-high SRP

treatment (Table 2), indicating coprecipitation is probably accounting for ~25% of the P removal in the high Ca/alk treatments. The P removal mechanisms (biological uptake and chemical coprecipitation) within the high Ca/alk-high SRP treatment microcosms yielded effluent SRP, TSP, and TP concentrations that approached those in the outflows of the treatments receiving no SRP amendments (Table 2 and Figure 2).

Beginning on December 29, 2000, the outflow pH values in the high and low SRP treatments receiving Ca and alkalinity amendments began to diverge (Figure 3). Although the outflow pH in both sets of treatments began to increase on that date, the higher pH values tended to be more associated with the high SRP treatment. A similar trend, corresponding to the same time period, also occurred in both sets (high and low SRP) of the unamended Ca/alk treatments (Figure 3). The most likely explanation for the higher pH values associated with the effluents of the SRP-amended treatments is the change in the nutritional status of the *Najas*. Initially, the P content of the *Najas* inoculated into all the treatments was 1306 mg/kg. After 8 weeks of exposure (prior to December 29, 2000) to SRP concentrations of 5 and 9 µg/L in the inflow waters, the *Najas* in the high and low Ca/alk-low (unamended) SRP treatment microcosms became P “deficient”. By contrast, the *Najas* in the microcosms receiving the amended SRP concentrations of 99 and 125 µg/L became P “enriched”. The result of the different P treatments is that after 8 weeks of exposure, the *Najas* populations receiving the higher SRP concentrations are capable of photosynthesizing more than the populations growing in low SRP medium, regardless of whether they are growing in high or low Ca/alkalinity water.

The enhanced pH elevation measured in the high Ca/alk-high SRP microcosms after December 29th corresponded to an increased reduction in the calcium and alkalinity concentrations within the high Ca/alk-high SRP microcosms compared to the low Ca/alk-high SRP microcosms (Figures 4 and 5). This was probably caused by the higher CaCO₃ saturation conditions in the inflow to the high Ca/alk-high SRP microcosms.

In conclusion, the preliminary findings for Experiment 2 of the P-coprecipitation subtask (5i) are in general agreement with the results reported from Experiment 1 of this subtask (DBE 2000). That is, depending on the initial SRP (and TSP), alkalinity, and hardness concentrations, and the

nutritional status of the SAV, coprecipitation of soluble P compounds and ions can occur, but this process accounts for less P removal than biological uptake by the SAV and/or bacterial communities.

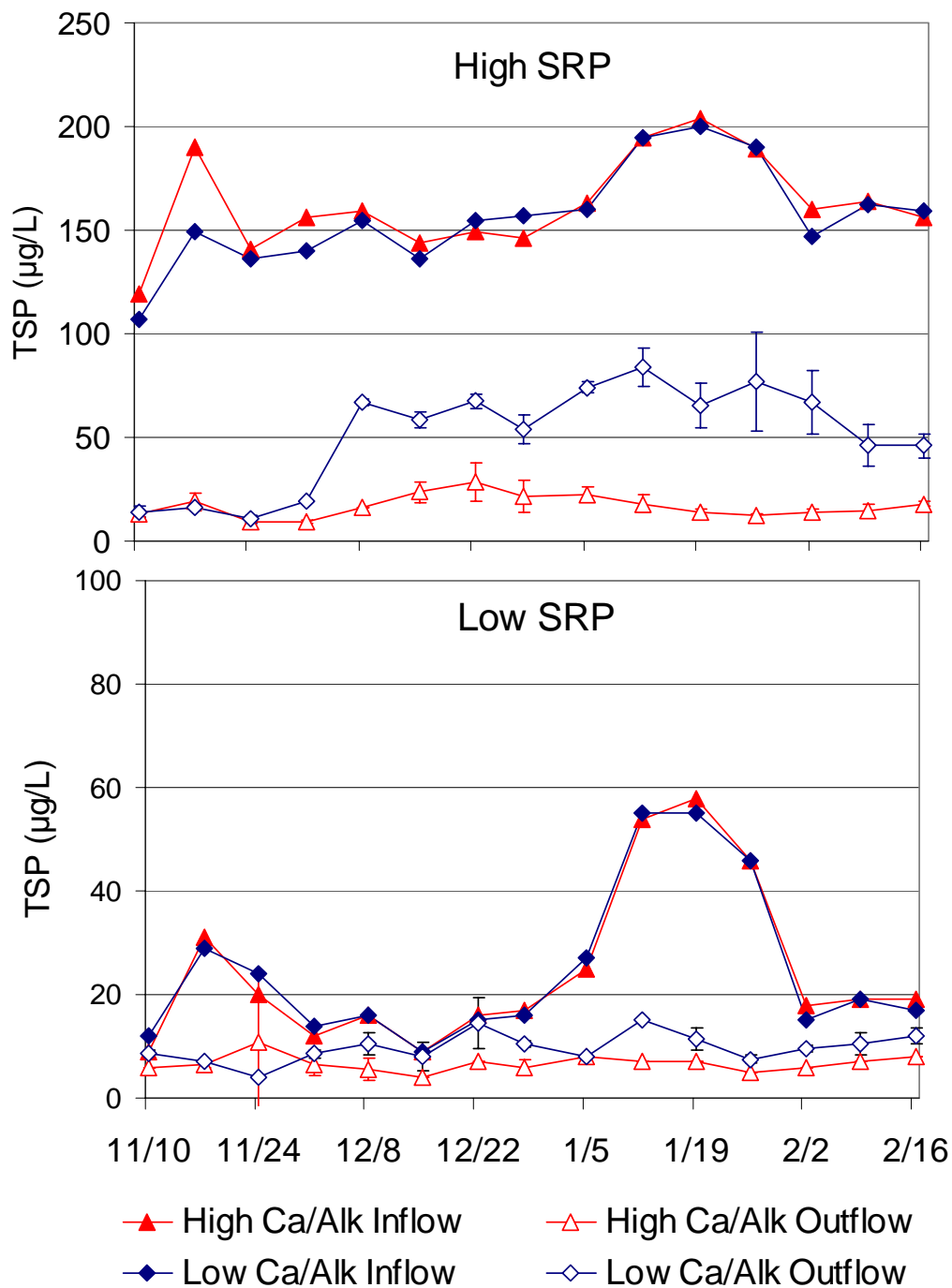


Figure 2. The total soluble P concentrations in the inflows and outflows of culture tanks containing *Najas* exposed to low and high calcium and alkalinity treated culture media with and without added (160 µg/L) soluble reactive P (SRP).

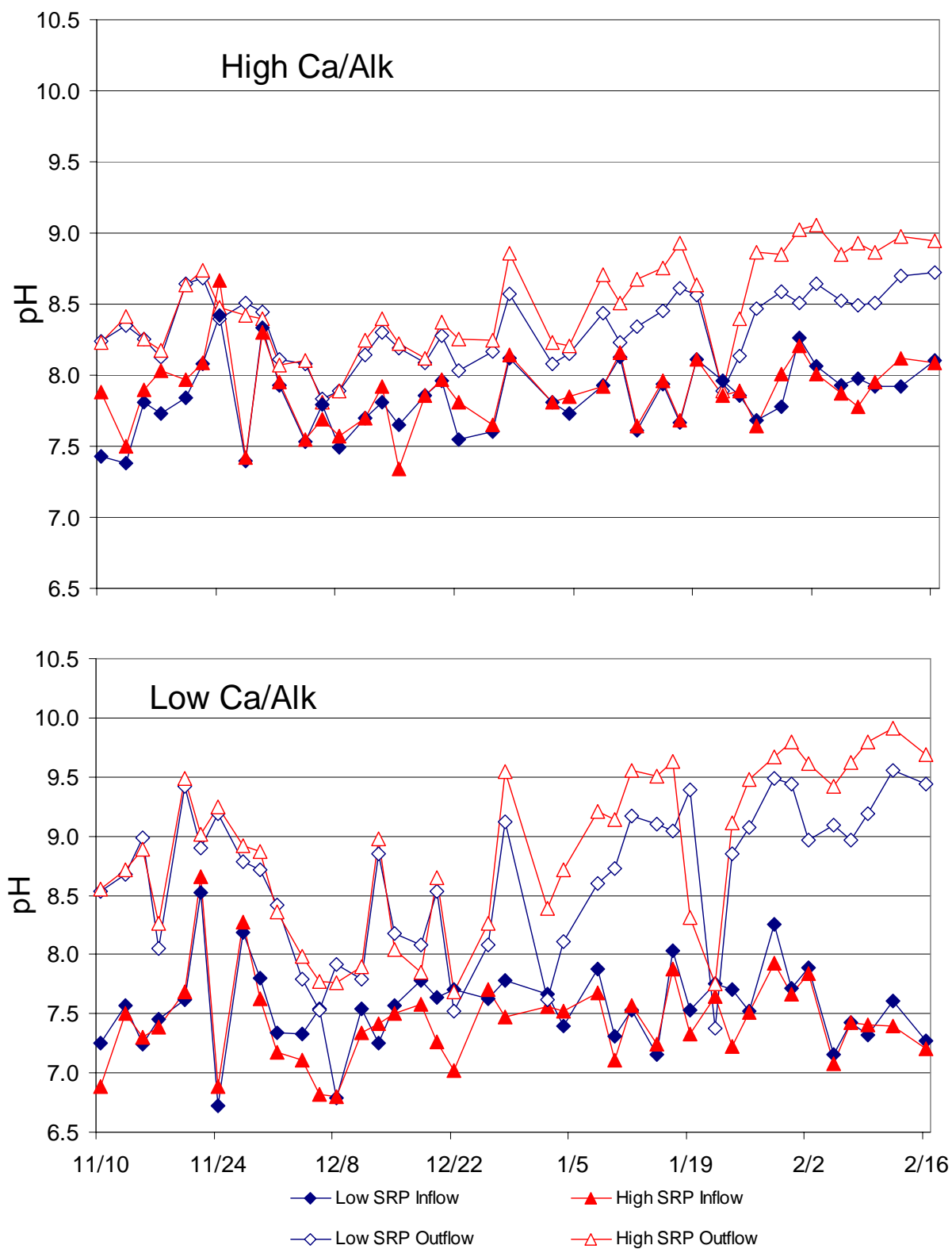


Figure 3. The pH values of the inflows and outflows of high and low calcium and alkalinity treated culture media with and without added (160 µg/L) soluble reactive P (SRP).

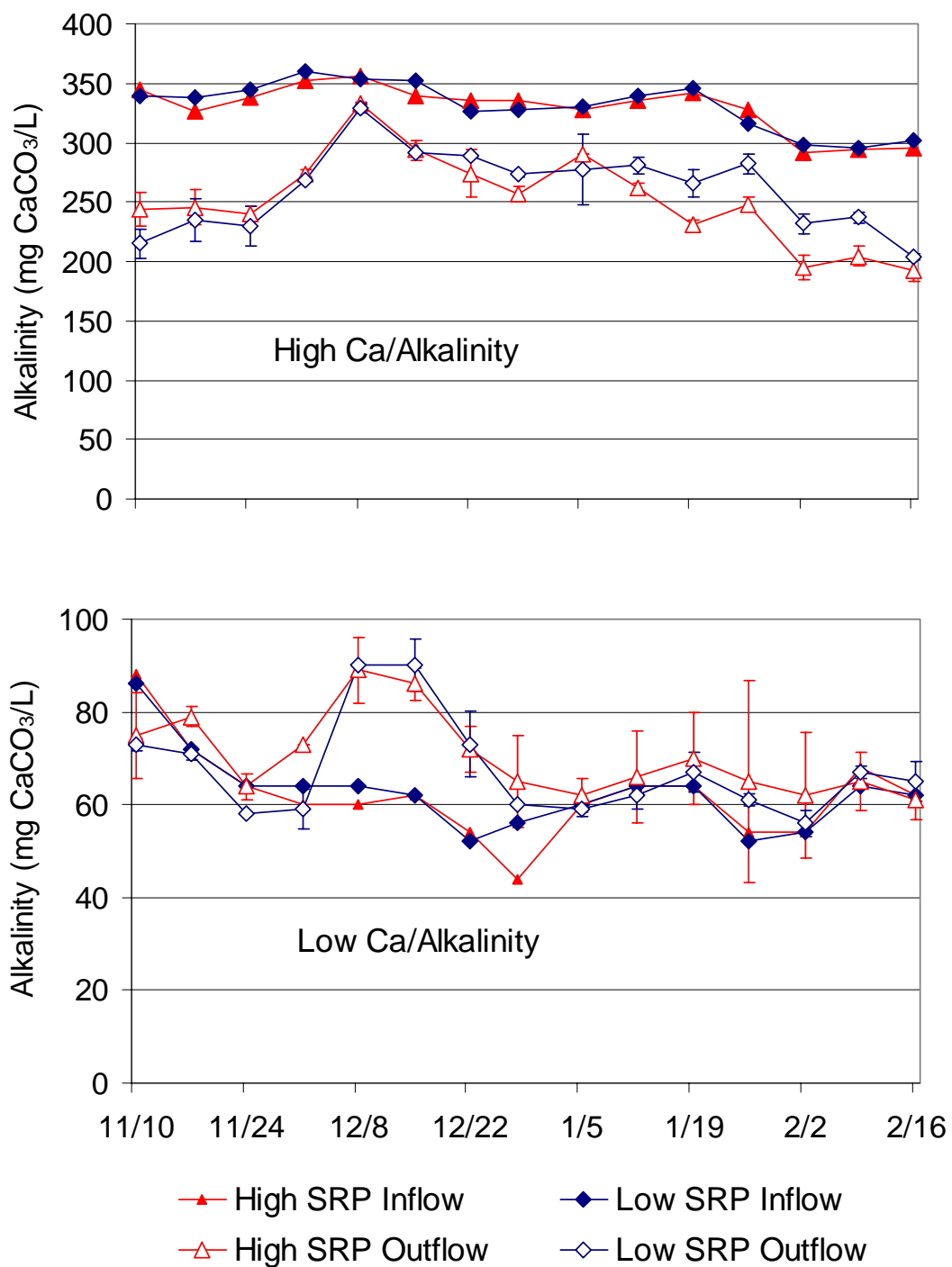


Figure 4. Total alkalinity concentrations in the inflows and outflows of culture tanks containing *Najas* exposed to SRP amended (160 $\mu\text{g P/L}$) and unamended culture media under high and low calcium and alkalinity concentrations.

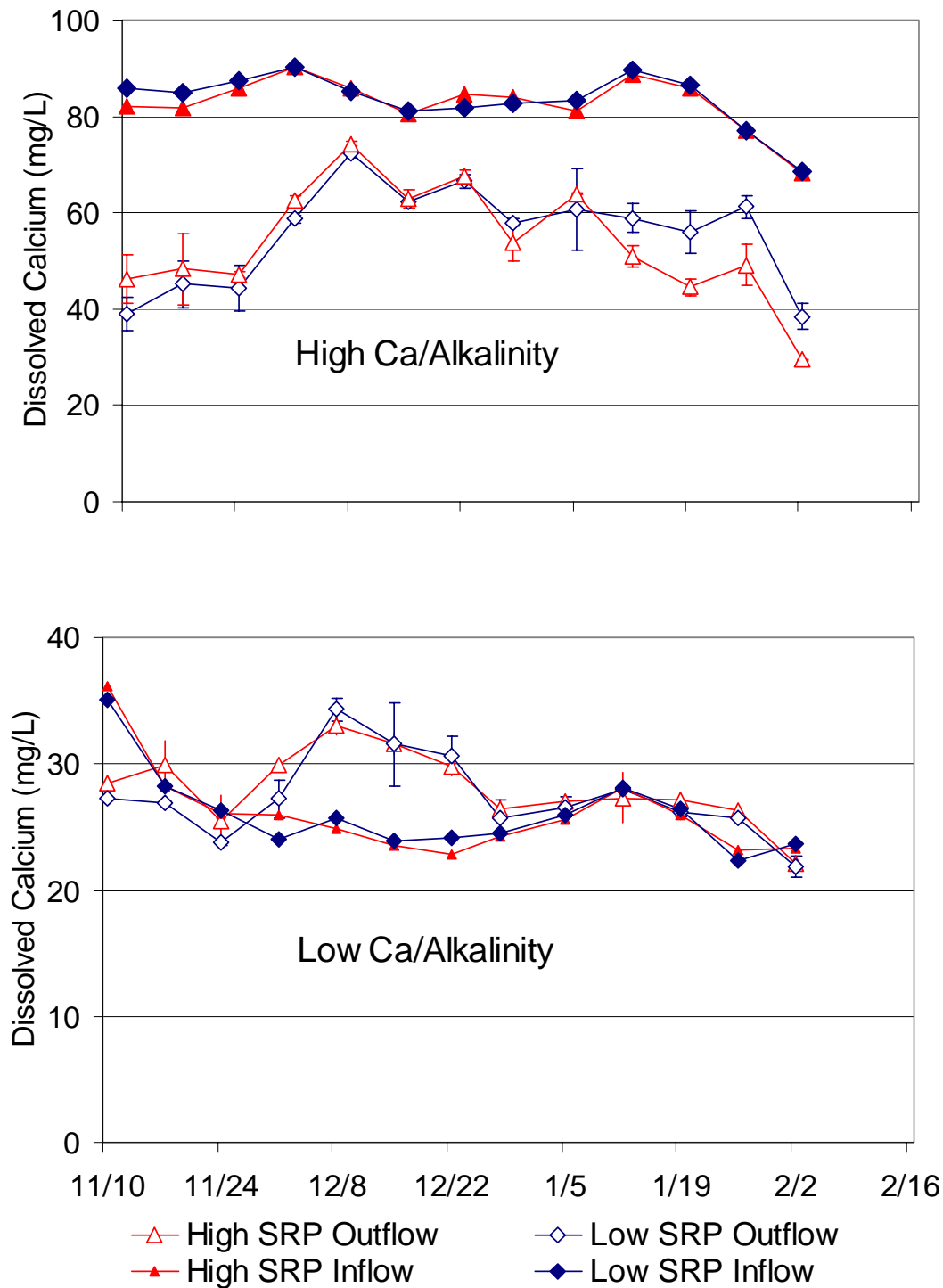


Figure 5. Dissolved calcium concentrations in the inflows and outflows of culture tanks containing *Najas* exposed to SRP amended (160 $\mu\text{g P/L}$) and unamended culture media under high and low calcium and alkalinity concentrations.

Long-Term Monitoring of P Removal Performance by SAV Mesocosms (Subtask 5iv)

Since June 1998, we have continuously operated three NATT site mesocosms at hydraulic retention times (HRT) of 1.5, 3.5 and 7.0 days. Inflow TP concentrations were lower than average during the most recent quarter (November 2000-January 2001), which resulted in below-average mesocosm outflow TP concentrations (Table 3). Limerock columns receiving mesocosm outflow continued to reduce total P concentrations, while also converting particulate P (PP) to SRP (Figure 6).

Table 3. Total phosphorus concentrations ($\mu\text{g/L}$) in the inflows, SAV outflows and limerock (LR) outflows of mesocosms operated at hydraulic retention times (HRT) of 1.5, 3.5 and 7.0 days since June 1998.

Period of Record	Inflow	1.5-Day HRT Outflow		3.5-Day HRT Outflow		7.0-Day HRT Outflow	
		SAV	LR	SAV	LR	SAV	LR
June 1998 – January 2001	99	51	40	31	21	25	18
November 2000 – January 2001	43	38	26	20	17	21	18

Despite the low ($43 \mu\text{g/L}$) inflow TP concentrations during the last quarter, TP concentrations in the LR outflows from the 3.5- and 7.0-day HRT systems were similar to average concentrations for the entire period of record (Table 3). This is due, in part, to recalcitrant DOP compounds either passing through or being generated within the SAV beds (Figure 6).

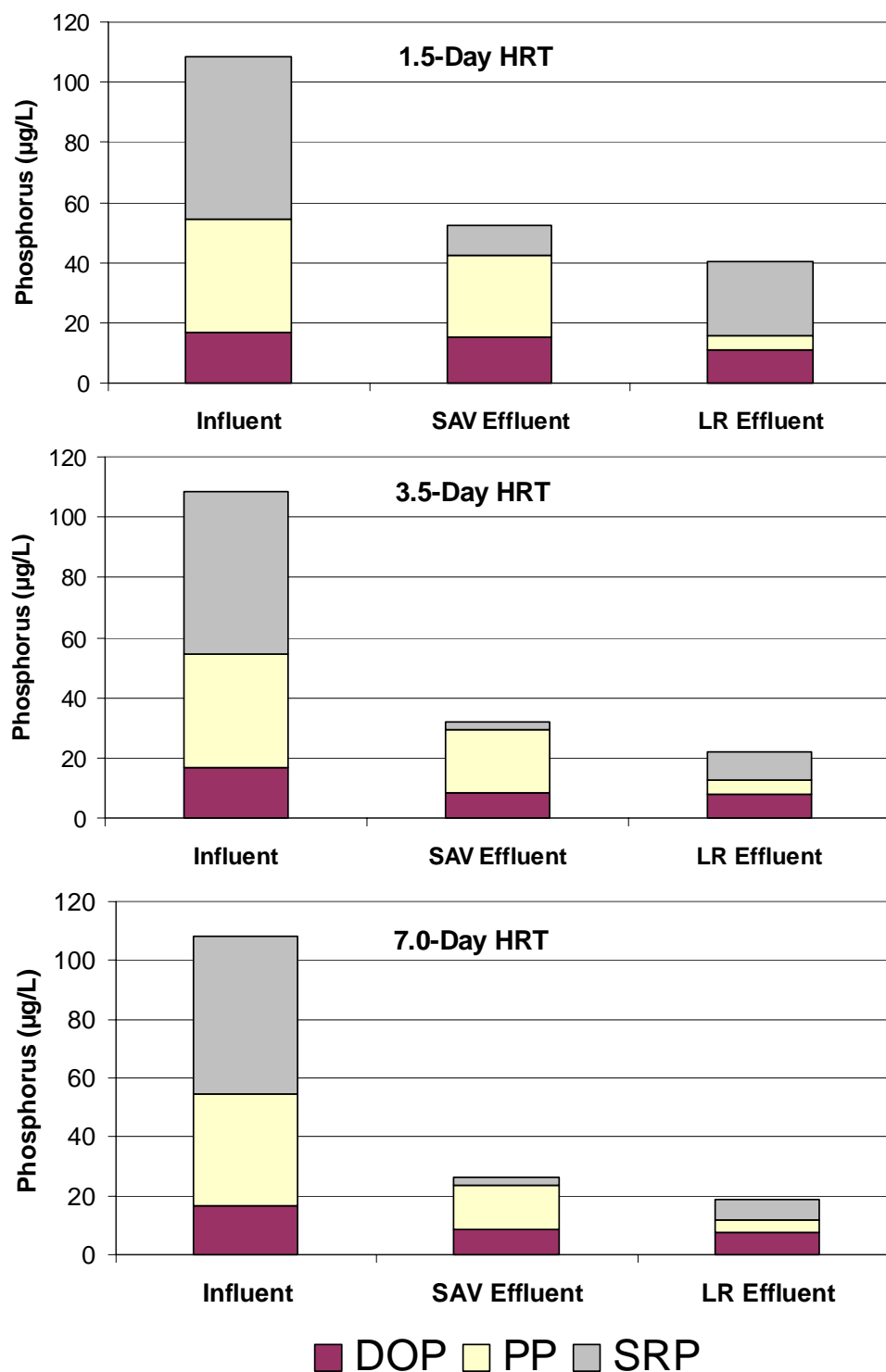


Figure 6. Mean soluble reactive, particulate, and dissolved organic phosphorus concentrations in the inflow and outflow from SAV mesocosms and outflow from subsequent limerock filters. SAV systems were operated at HRTs of 1.5, 3.5 and 7.0 days, while each LR filter had an HRT of 5 hours.

Effects of Pulse Loading on Phosphorus Removal Performance by SAV Communities (Subtask 5v)

During the 40-week experimental period that began February 20, 2000, we operated six mesocosms under variable hydraulic loading rates that were based on flow data from STA-2 (Table 4). Hydraulic loading rates (HLR) in duplicate mesocosms were scaled to correspond with 11, 23, and 53 cm/day HLRs used in the HRT study (Subtask 5iv) “control” mesocosms. The investigation, concluded on November 24, 2000, culminated with two weeks of zero flow, the seventh such “no-flow” period during the study (Table 4).

Table 4. Forty-week (Feb. 20 - Nov. 24, 2000) pulse loading schedule for low, medium, and high loaded mesocosms. The shaded section of the table corresponds to the current reporting quarter.

Week	Loading schedule (cm/day)			Week	Loading schedule (cm/day)		
	Low	Medium	High		Low	Medium	High
1*	0	0	0	21	13.2	26.4	66
2	0	0	0	22	13.2	26.4	66
3	22	44	110	23	44	88	220
4	22	44	110	24	44	88	220
5	4.4	8.8	22	25	0	0	0
6	4.4	8.8	22	26	0	0	0
7	0	0	0	27	26.4	52.8	132
8	0	0	0	28	26.4	52.8	132
9	13.2	26.4	66	29	8.8	17.6	44
10	13.2	26.4	66	30	8.8	17.6	44
11	0	0	0	31	35.2	70.4	176
12	0	0	0	32	35.2	70.4	176
13	0	0	0	33	6.6	13.2	33
14	0	0	0	34	6.6	13.2	33
15	26.4	52.8	132	35	11	22	55
16	26.4	52.8	132	36	11	22	55
17	0	0	0	37	22	44	110
18	0	0	0	38	22	44	110
19	17.6	35.2	88	39	0	0	0
20	17.6	35.2	88	40**	0	0	0

* Beginning week for Pulse Loading experiment: Feb. 20, 2000

**Termination of experiment: Nov. 24, 2000

Outflow region water quality was monitored throughout these quiescent periods and was typified by below average TP in the low load mesocosms (Table 5; Figure 7) and equal TP (to flow-thru conditions) in the moderate load mesocosms (Table 5; Figure 8), but higher-than-average TP concentrations in the high load mesocosms (Table 5; Figure 9). As previously

reported (DBE 2000), we attributed this phenomenon to phytoplankton growth in the stagnant, high-loaded water column, which would have received a higher internal loading during the quiescent period than the low-load mesocosms. Once flows were resumed, SAV outflow TP concentrations rapidly returned to levels observed prior to the no-flow period (Figure 9). Phytoplankton “washout” and removal of P diffusion gradient limitations on macrophyte P uptake may be possible reasons for the transient nature of the elevated TP concentrations observed during periods of zero flow.

Table 5. Average total phosphorus concentrations in the water column (outflow region) of NATT site pulse loaded mesocosms, during quiescent (7 two-week periods) and flowing (13 two-week periods) conditions.

	Low Load	Medium Load	High Load
Quiescent Average TP	28	45	93
Flowing Average TP	32	45	67

Total P concentration reductions in high flow mesocosms (mean HLR = 53 cm/day) were greater in the control mesocosms than in the pulsed systems (52% vs. 37%), indicating pulsing had a negative effect on P removal efficiency. However, this pulsing effect decreased with reduced loading – there was little difference in performance between pulsed and control moderate- and low-flow treatments (Figures 7 and 8). Because the HLRs tested during this study (0-220 cm/day) are as much as two orders of magnitude greater than the “design” HLR for an STA (mean (max.) HLR for STA-1W = 2.3 (53) cm/day), the reduced performance observed under “high” pulsed flows is not likely to occur in a full scale system. These trends suggest that pulsed loading may affect performance in the inflow region of a full-scale treatment cell, but little or no effect would be detected at the outflow region under current design HLRs of 2.3 cm/day.

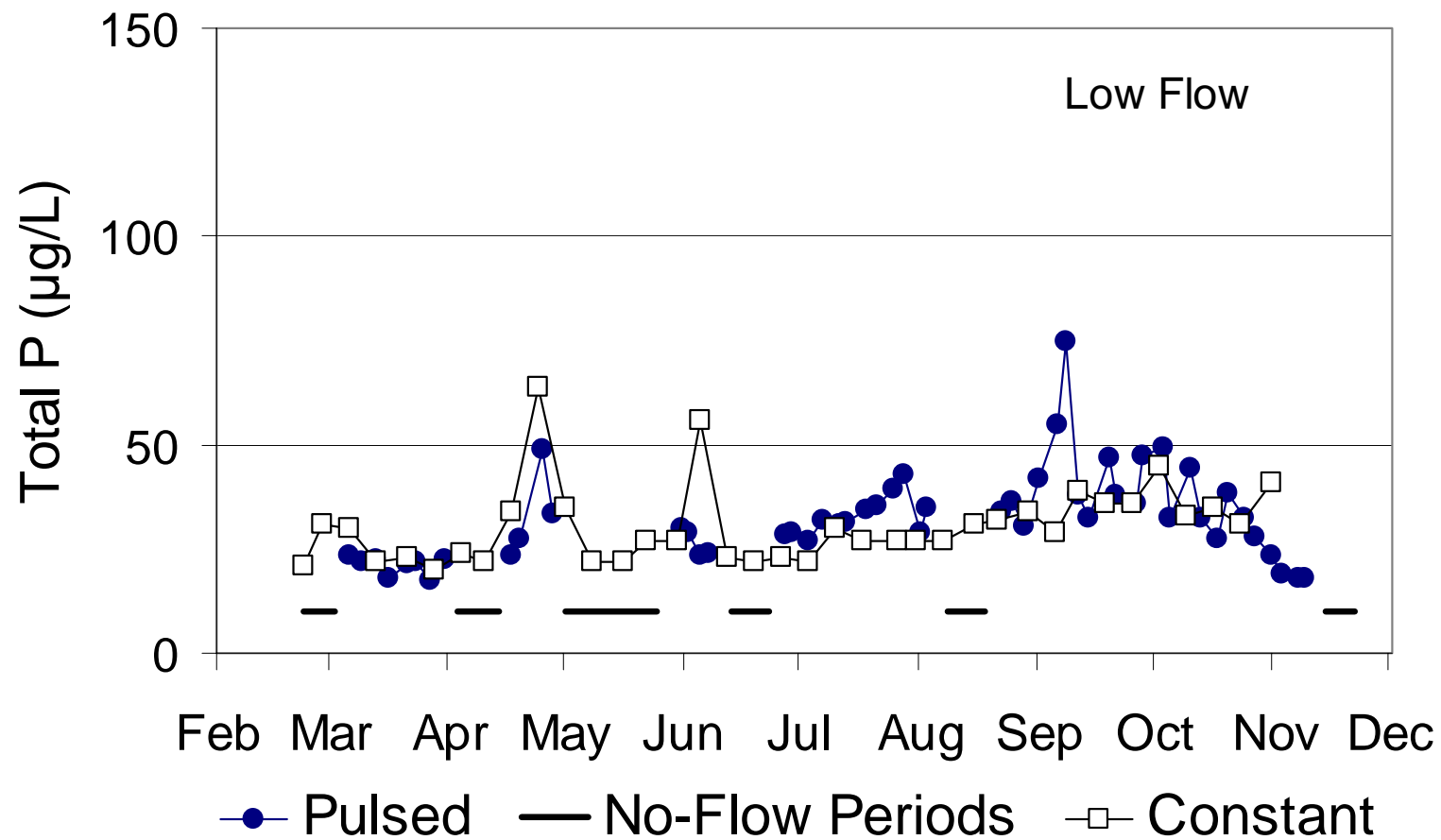


Figure 7. Mean outflow total P concentrations in duplicate pulse loaded mesocosms compared to a constant load mesocosm operated at a similar average hydraulic loading rate of 11 cm/day. Periods of no flow to the pulsed systems are denoted by horizontal lines.

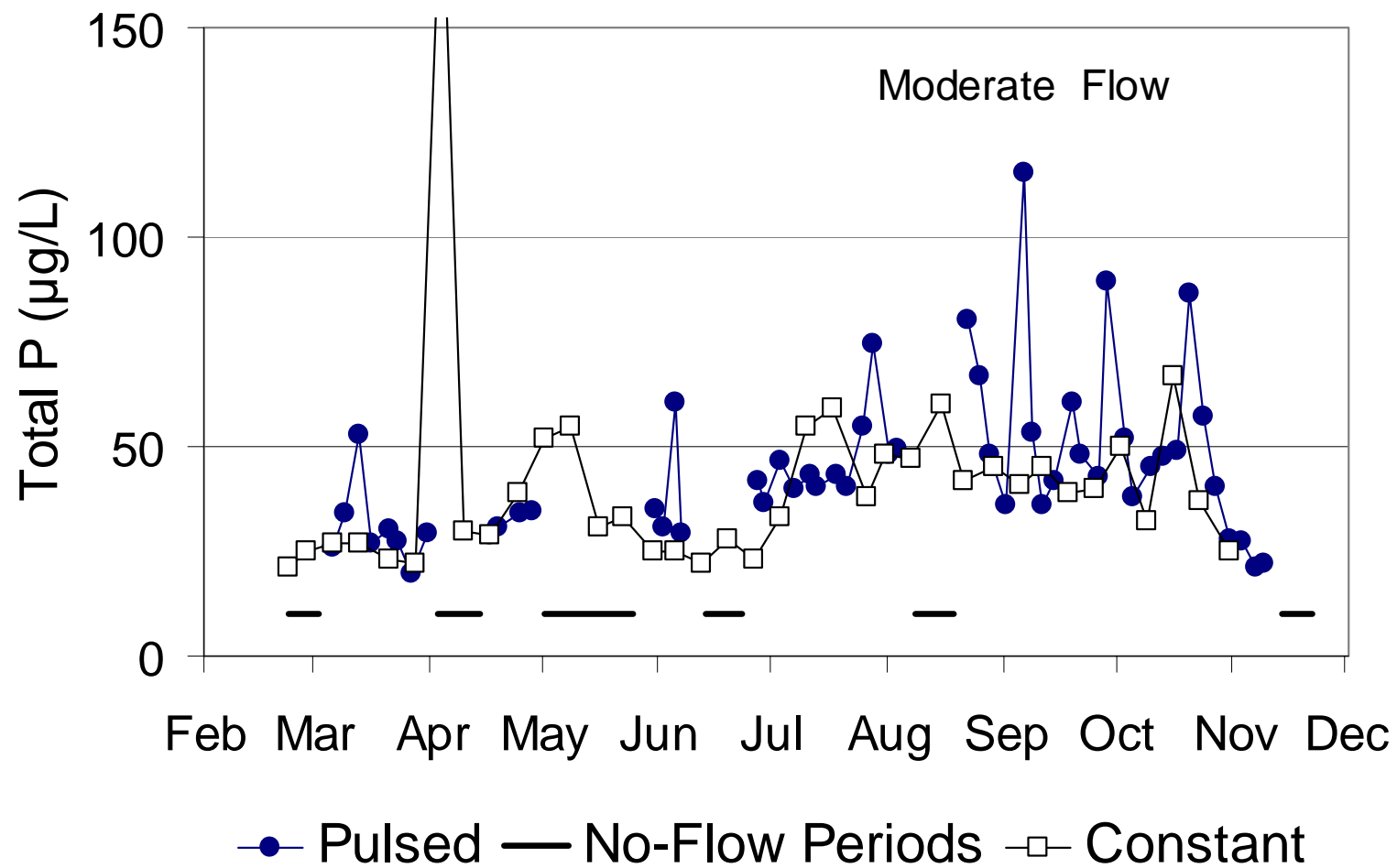


Figure 8. Mean outflow total P concentrations in duplicate pulse loaded mesocosms compared to a constant loaded mesocosm operated at a similar average hydraulic loading rate of 23 cm/day. Periods of no flow for the pulsed systems are denoted by horizontal lines.

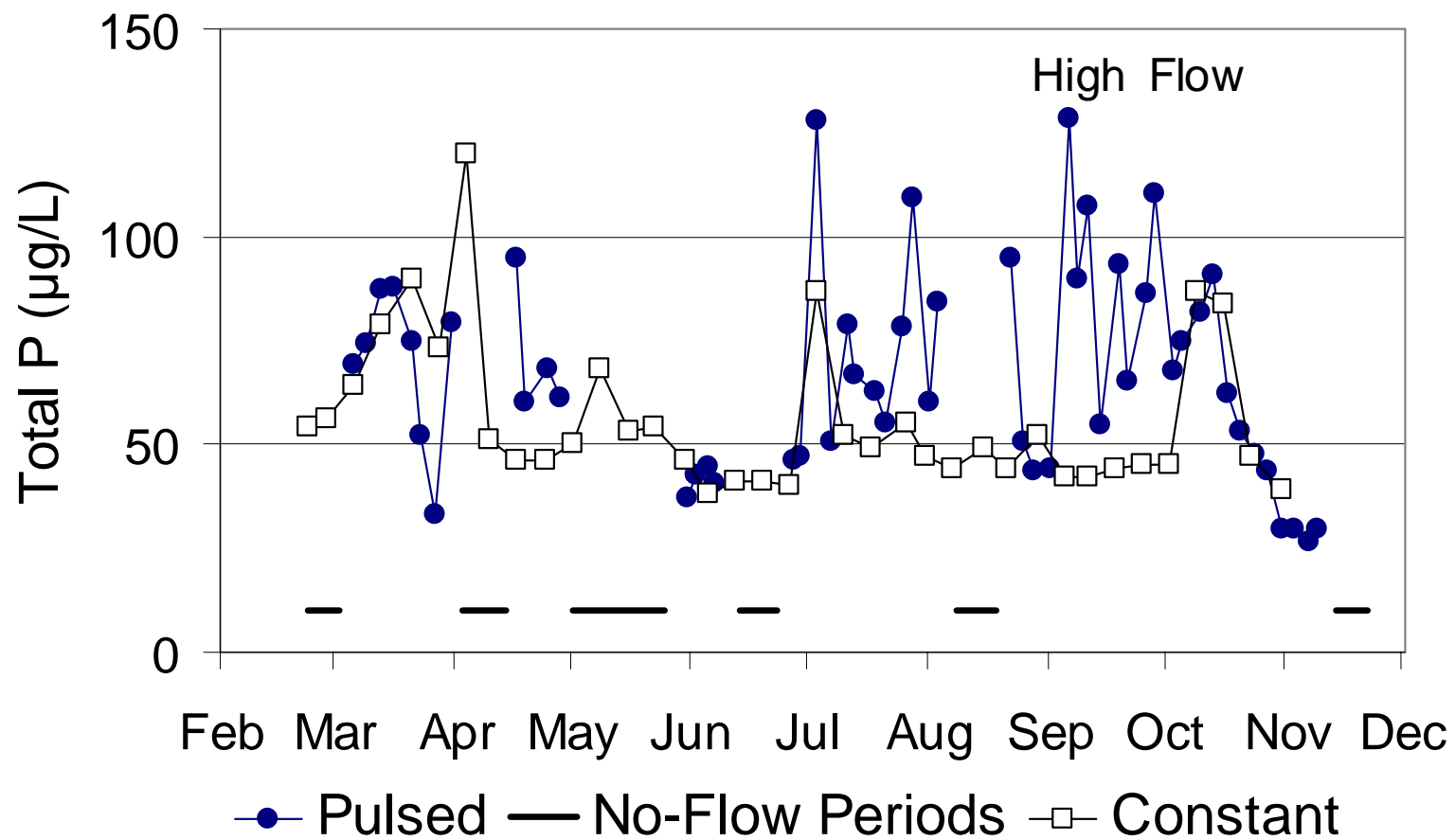


Figure 9. Mean outflow total P concentrations in duplicate pulse loaded mesocosms compared to a constant loaded mesocosm operated at a similar average hydraulic loading rate of 53 cm/day. Periods of no flow for the pulsed systems are denoted by horizontal lines.

Effects of Dryout and Reflooding on Phosphorus Retention (Subtask 5v)

Upon completion of the Pulse Loading study (November 24, 2000), we began a dryout-reflooding investigation in two of the six pulsed mesocosms (one each of the high and low flow treatments). This effort began with “baseline” water sampling at the inflow and outflows of the SAV and LR unit processes. During the six weeks of baseline sampling the two mesocosms received Post-BMP waters at constant HLRs of 11 and 53 cm/day. Inflow – outflow TP, pH and temperature measurements were performed weekly. Total soluble P (TSP), soluble reactive P (SRP), dissolved calcium and total alkalinity were measured on biweekly composites of weekly grabs.

As was reported for the Long-Term Monitoring (Subtask 5iv) investigation, TP concentrations were reduced more within the lower loaded mesocosms (L-3) than the higher loaded mesocosms (S-3) (Table 6). Slight increases in SRP concentration for both mesocosms occurred within the LR beds. The LR bed was particularly effective in removing the PP leaving the high HLR (53 cm/day) mesocosm. DOP remained at the same concentration as the inflow concentration throughout the “high-flow” processes, whereas we observed a 50% reduction in DOP in the lower loaded mesocosm (Table 6).

Table 6. Chemical characteristics of the inflows and outflows of mesocosms receiving high (53 cm/day) and low (11 cm/day) HLRs, and of outflows from downstream limerock barrels, during a six week baseline monitoring period prior to dry-down. Values represent means of six weekly grabs (TP, SRP, pH) or three two-week composites (DOP, PP, alkalinity).

Hydraulic Load	Inflow		SAV Outflow		LR Outflow	
	High	Low	High	Low	High	Low
TP (µg/L)	50	51	44	15	31	17
SRP (µg/L)	28	28	17	2	19	4
DOP (µg/L)	11	11	10	5	9	5
PP (µg/L)	10	12	17	8	2	8
Alk (mg CaCO ₃ /L)	197	196	193	135	193	161
Diss. Ca (mg/L)	63	64	64	41	65	49
pH	7.68	7.83	8.05	8.98	7.80	8.01

After the six-week baseline monitoring, the water level in both mesocosms was reduced from 0.8 to 0.3 m. Small (0.30 m²) quadrats were sampled in the inflow and outflow regions of each

mesocosm to characterize the vegetation standing crop (wet and dry) and to quantify the plant N, P and Ca contents.

Vegetation was removed from the center cross-section of each tank by clipping and removing the above-sediment canopy to facilitate core retrieval, and the water level was reduced to 1 cm to initiate the dryout period. Triplicate sediment cores (15.9 cm² each) were collected from this exposed central region after 0, 7 and 14 days had elapsed. The accreted sediment layer, which was easily identified from the underlying peat, was extruded in one of the three cores and immediately dried for moisture content calculations.

The other two intact cores retrieved from each mesocosm were re-flooded with 250 mL Cell 4 inflow water (stored in the dark at 4°C between trials), and laboratory-incubated in the dark in a water bath (26 ± 1°C) for 24 hours. Initial conditions in the overlying water are provided in Table 7. A control core (identical acrylic core with 250 mL overlying water and without sediment) was also incubated with the four sediment cores during each trial. Moisture content and Ca and P concentrations of each sediment core will be measured to compare with SRP release data.

Table 7. Characteristics of incubation overlying water collected from Cell 4 Inflow on January 10, 2001.

	pH	TP	SRP	DOP	PP	Alkalinity	Ca
Cell 4 Inflow	7.81	36	14	13	9	302	81.6

Immediately after draw-down ($\Delta T = 0$ days), overlying water SRP concentrations were reduced from 14 µg/L to below the method detection limit (MDL) of 2 µg/L in cores retrieved from the low loading mesocosm (L-3). In contrast, SRP concentrations were relatively unchanged in the high loading mesocosm (S-3) cores (11 ± 4 µg/L). Control overlying water (no sediment) was reduced from 14 to 6 µg SRP/L during the 24 hr incubation. During the $\Delta T = 7$ day post-desiccation 24-hour core incubations, SRP concentrations were reduced from 13 to ≤ 3 µg/L in S-3, L-3 and control (overlying water only) cores. At $\Delta T = 14$ days, however, differences were again observed between treatments. SRP concentrations increased from 14 to 57 µg/L in the

overlying water of the S-3 sediment, while L-3 sediment and control overlying water were reduced to 2 µg SRP/L.

The pH values increased equally across all treatments during each trial. Initial pH values of 7.81 – 7.93 increased to 8.52 - 8.85 after 24 hours. Moisture content remained unchanged since the beginning of the desiccation period, with $88 \pm 2\%$ water found in cores across all treatments (S-3 and L-3) and trials ($\Delta T = 0, 7$ and 14 days).

Phosphorus release from drying sediments is expected *a priori* to be greater from S-3 sediments than from L-3 sediments, due to higher TP and lower TCa concentrations in the former (DBE 2001). Sediments formed under higher nutrient loadings (such as S-3 and Cell 4 Inflow) exhibit higher TP and organic matter concentrations and lower Ca concentrations. They consequently release more P upon reflooding when compared to sediments formed under lower nutrient loadings (L-3 and Cell 4 Outflow).

After the dryout (minimum six weeks), the mesocosms (and associated LR beds) will be reflooded, and P removal/export (from SAV and LR unit processes) will be assessed for 13 weeks. Outflow water samples will be collected more frequently during the first hours to characterize the potential first “flush” of P from the rehydrated sediments and vegetation. This protocol will enable us to assess the impact of sediment desiccation on P removal/export, to gauge the influence of previous P loading regime on sediment stability, and to evaluate the ability of the SAV communities to recover after the dryout event.

Comparison of Phosphorus Removal Performance by Cattail- and SAV-Dominated Systems (Subtask vi)

Superior performance by SAV-dominated systems over cattails has been demonstrated by this mesocosm-scale experiment, where one SAV- and two cattail-dominated mesocosms (water depth = 0.4 m) were hydraulically loaded at 10 cm/day. The SAV and cattail communities have provided average outflow TP concentrations of 25 and 53 µg/L, respectively, for the period December 29, 1998 to January 30, 2001 (Figure 10).

During this quarter, SAV- and cattail-dominated mesocosms reduced inflow TP concentrations by 60 and 32 %, respectively. Particulate P and SRP concentrations were lower in the SAV outflow than in the cattail outflow, while DOP concentrations remained constant through the cattail-dominated system and decreased in the SAV mesocosm (Figure 11).

Shallow Low Velocity SAV/Periphyton/Limerock Systems (Subtask 5vii)

Monitoring of the triplicate shallow periphyton-dominated raceways was concluded November 28, 2000, after continuous operation for 29 months (Figure 12). The raceways reduced average TP concentrations in the Post-STA waters from 21 to 12 µg/L, and back-end limerock filters provided further removal to 10 µg/L over the entire period of record. Hydraulic loading to the raceways ranged from 10 to 22 cm/day, which provided an average mass P removal of 0.34 gP/m²/yr. This system demonstrated that at the mesocosm scale, a “green” SAV/periphyton-based technology is capable of reducing TP concentrations to the target 10 µg/L on a long-term basis.

Effects of Flow Velocity on Phosphorus Removal by Shallow SAV/Periphyton Communities (Subtask 5viii)

Many investigators believe that flow velocity is an important variable in controlling the performance of SAV and periphyton systems. This parameter is difficult to test at the mesocosm scale, however, because any increase in flow (to increase velocity) also results in an increase in P loading. Also to adequately address the effect of flow velocity on P removal using mesocosms, a long experimental platform is required.

Upon completion of the shallow, low velocity periphyton/LR study (Subtask 5vii) on November 28, we joined the three 44 m long raceways together in series, thereby tripling the length of the flow path (Figure 13). We also tripled the inflow hydraulic loading rate to 66 cm/day, providing a velocity of 0.36 cm/sec. This flow rate is in the middle of the mean velocity range (0.2-0.5 cm/sec at average flow) proposed for the STAs. We will analyze inflow and outflow waters weekly for TP for a six month period under this modified operational regime.

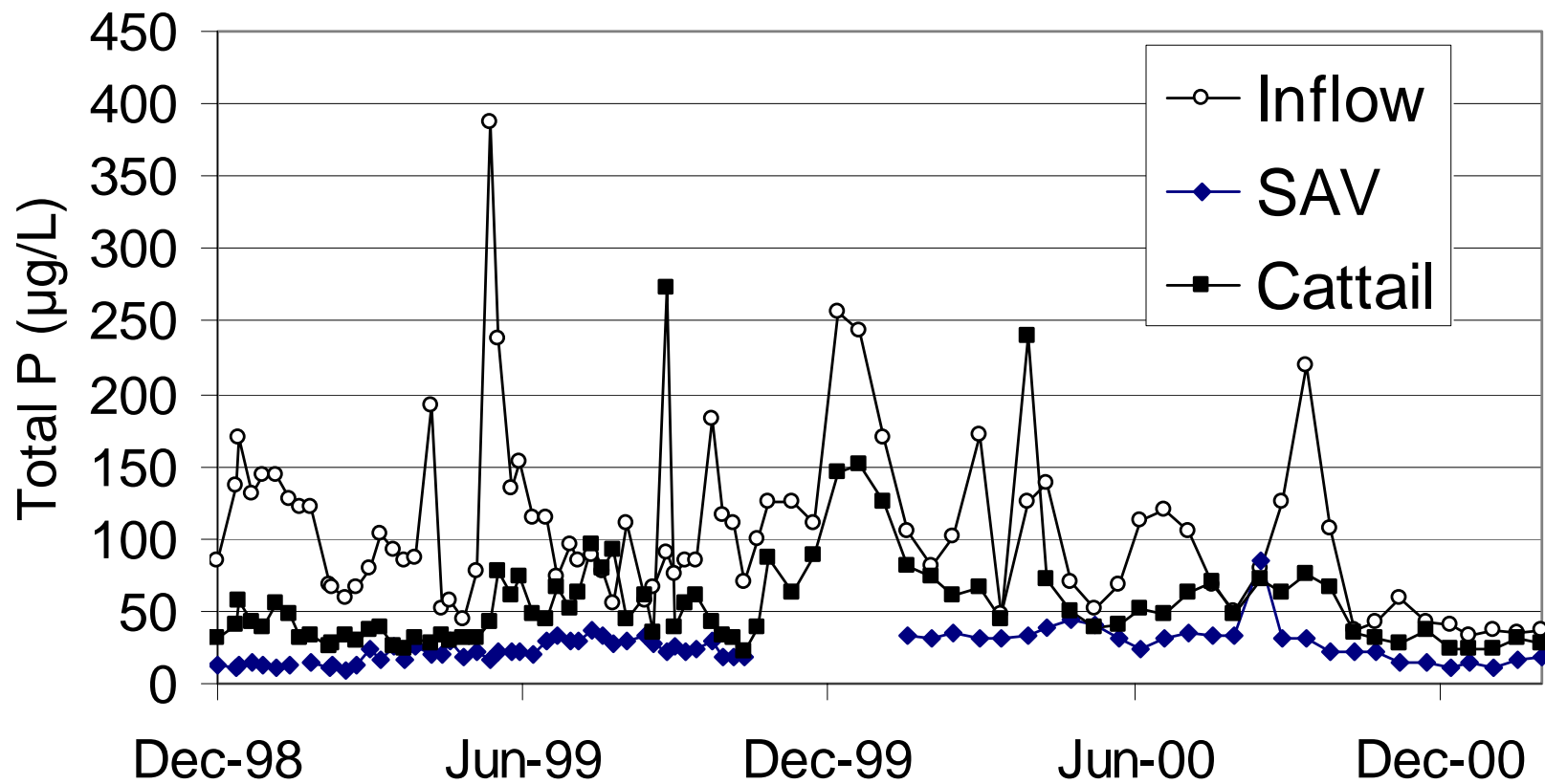


Figure 10. Mean total phosphorus concentrations in the inflows and outflows from SAV- and cattail-dominated mesocosms operated since December 1998.

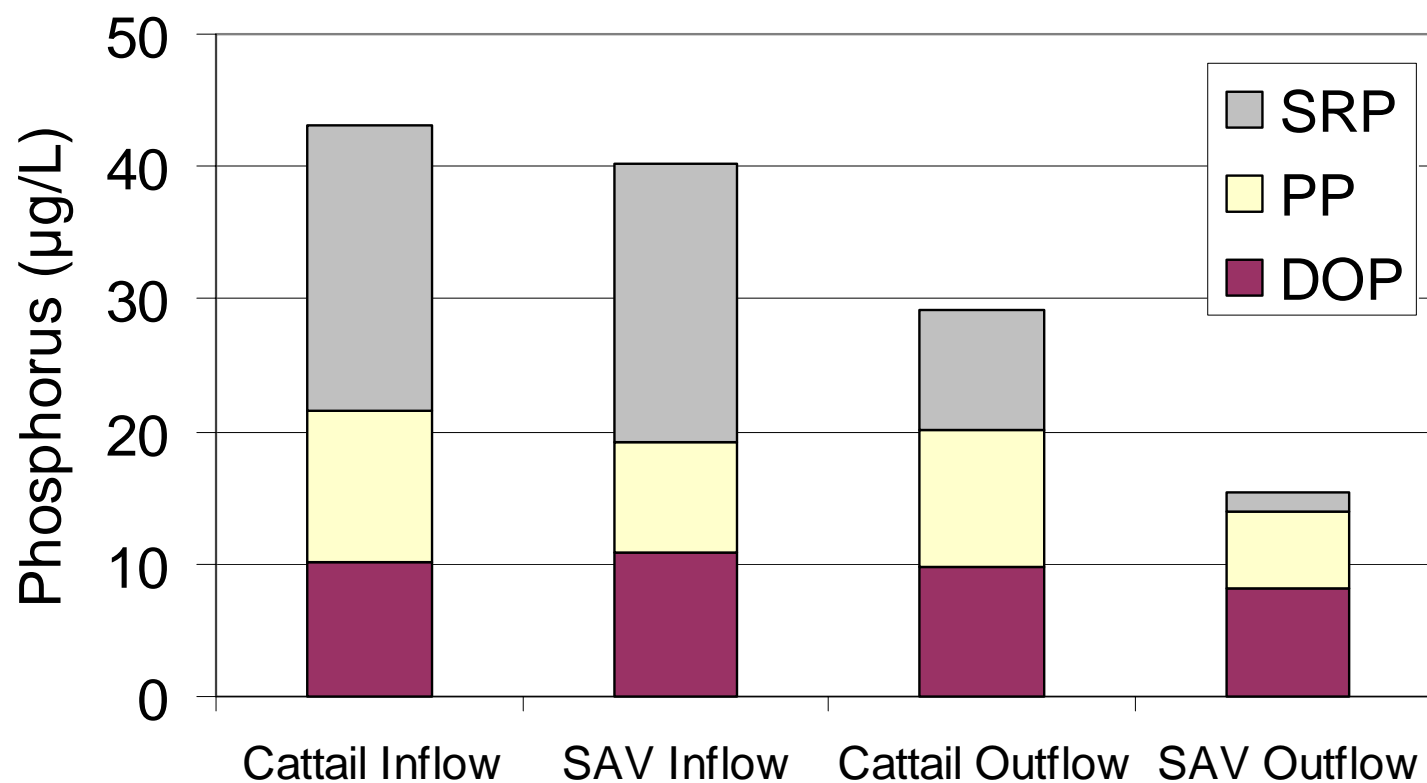


Figure 11. Mean soluble reactive, particulate and dissolved organic phosphorus concentrations in the inflows and outflows from SAV- and cattail-dominated mesocosms during the November 2000-January 2001 quarter.

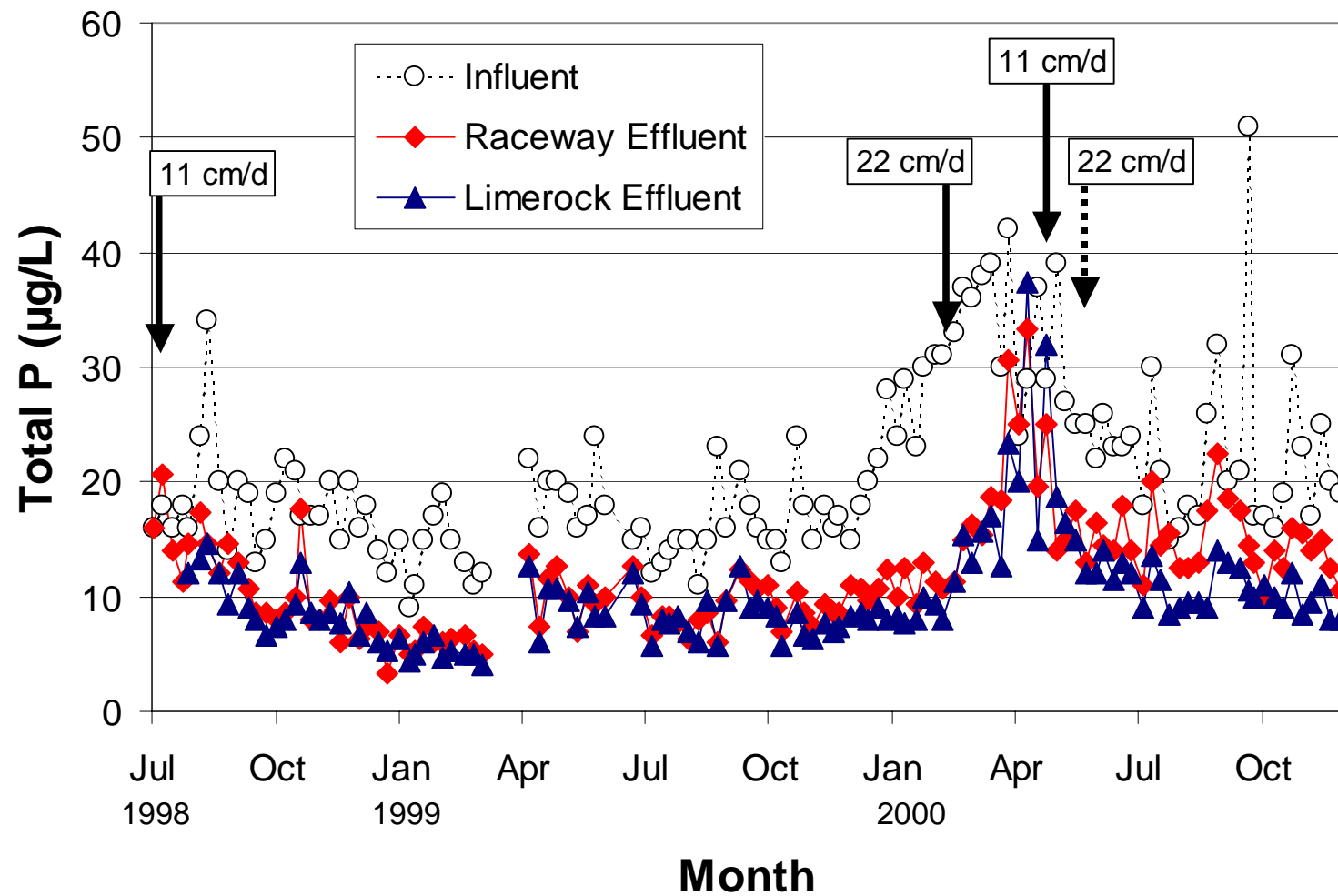


Figure 12. Total phosphorus concentrations in the inflow and outflows of triplicate shallow, low velocity, SAV/periphyton raceways and in the outflow of the subsequent limerock beds. Dates of flow manipulations are depicted on the figure. Values after the second 22 cm/day flow adjustment represent the means of duplicate raceways.

During the first ten weeks of high velocity operation, *Chara* has established dominance along the inflow region of the raceway, while calcareous periphyton dominates most of the remaining 132 m long raceway. A mixed *Chara* /periphyton community dominates certain sections of the raceway where the pre-existing community gradients developed under the previous parallel flow paths of Subtask 5vii. For this initial 10-week period, TP was reduced from an average inflow concentration of 19 µg/L to a raceway outflow of 16 µg/L (Figure 14). Concentrations were further reduced to 9 µg/L by the limerock filter.

Growth of SAV in Post-STA Waters on Muck, Limerock and Sand Substrates (Subtask 5ix)

Duplicate mesocosms (each with three tanks plumbed in series) established on muck, limerock and sand substrates have been operated at the SATT site since July 1999. Muck mesocosms have continually supported higher SAV biomass than the LR or sand mesocosms (pers. obs.). Differences in P removal performance were observed during prior periods, with muck and limerock outperforming the sand-based systems (Figure 15). These differences were absent, however, during the November 2000 - January 2001 quarter (Table 8): each substrate treatment reduced inflow TP concentrations by ~50%.

High Velocity
66 cm/day HLR

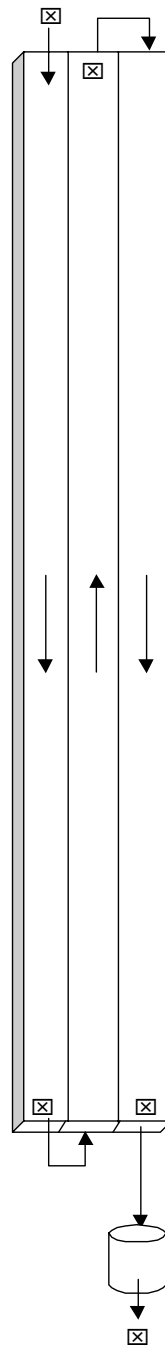


Figure 13. Sampling locations for the experiment on the effects of flow velocity on P removal by a shallow SAV/periphyton community.

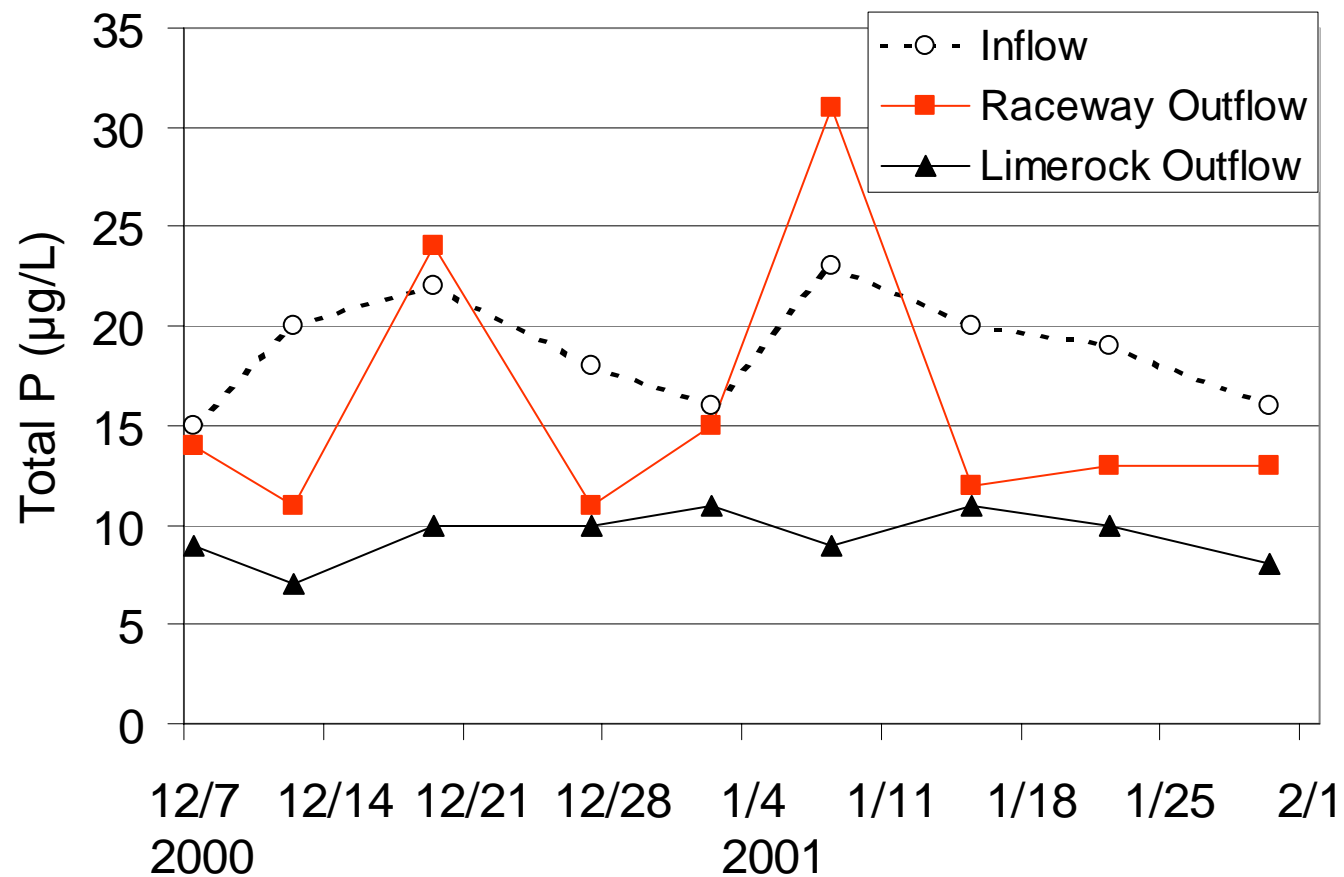


Figure 14. Total P concentrations in the inflow and outflow of a shallow (9 cm deep) raceway dominated by a mixed *Chara*/periphyton community and in the outflow of a subsequent limerock bed at a hydraulic loading rate of 66 cm/day (velocity = 0.36 cm/sec).

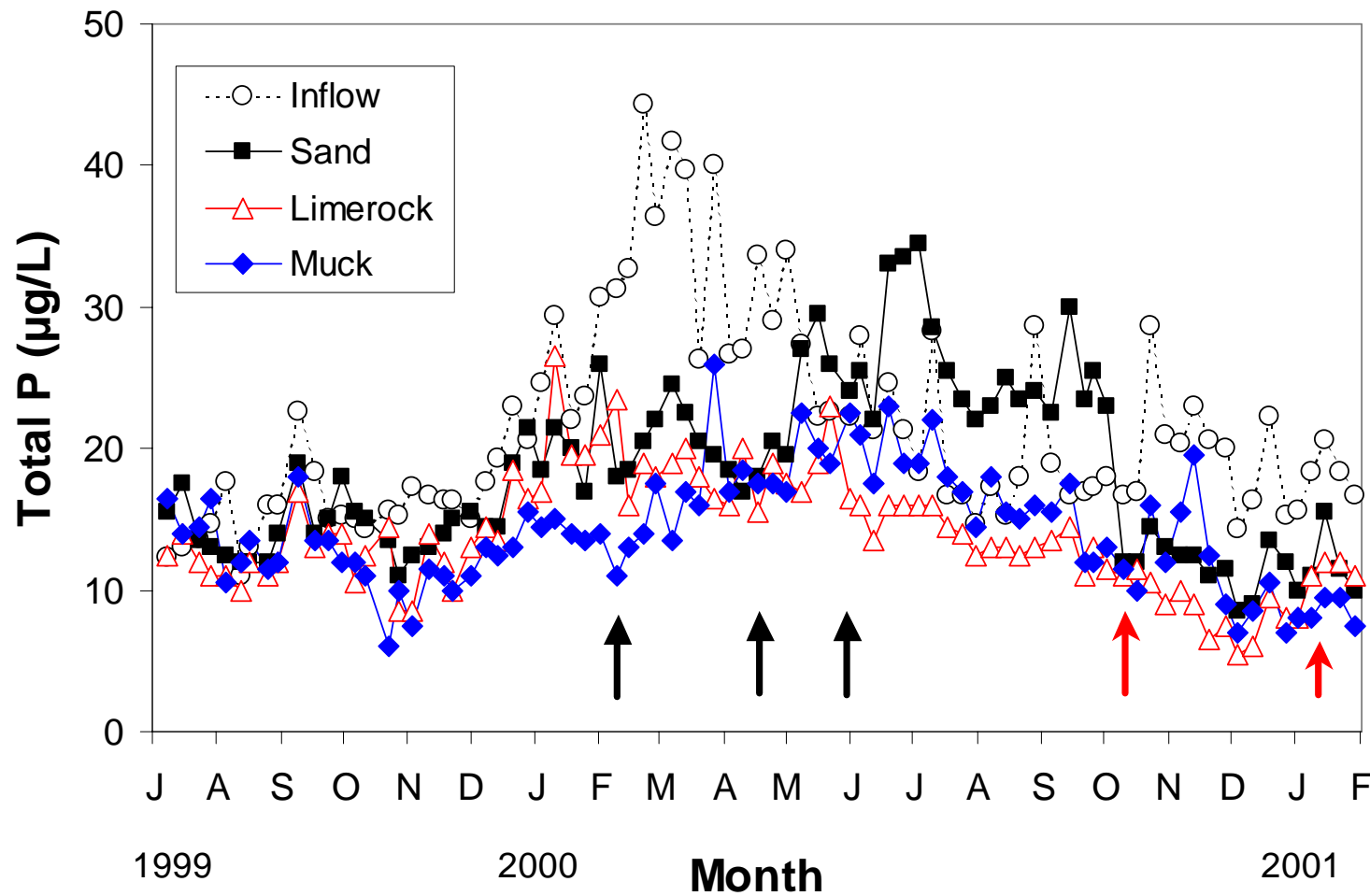


Figure 15. Mean total phosphorus concentrations in the inflow and outflows of duplicate SAV treatment trains operated on sand, limerock and muck substrates from July 1999 to March 2001. Black arrows denote 50% reduction of flows on February 9, April 17 and May 31 2000. The red arrows denote doubling of flows on October 10, 2000 and January 9, 2001.

Table 8. Mean (± 1 s.d.) total phosphorus concentrations in the inflow and outflows from SATT mesocosms established on muck, limerock and sand substrates during the two most recent quarters.

	Inflow	Muck	Limerock	Sand
August 2000 – October 2000	19 \pm 1	12 \pm 1	14 \pm 2	21 \pm 5
November 2000 - January 2001	19 \pm 1	9 \pm 1	10 \pm 1	11 \pm 1

Effects of Filter Media Size and Type on P Removal Performance (Subtask 5x)

Sampling of the sixteen filter column inflows and outflows was performed from August 18 to November 17, 2000. Total, total soluble, and soluble reactive phosphorus concentrations were analyzed as twice-weekly grab samples, while specific conductance, calcium and alkalinity samples were composited each week.

Mean inflow and outflow concentrations of TP, SRP, DOP, PP, Ca and alkalinity are presented in Table 9. Outflow TP concentrations were slightly lower for the limerock and Pro-Sil Plus™ (13 – 14 $\mu\text{g/L}$) than the quartz sand treatments (14 – 17 $\mu\text{g/L}$). There were no differences between coarse and medium size filter media in TP removal (Figures 16 - 18). The TP concentrations in the twice-weekly grabs varied less toward the end of the sampling period across all three substrates within each size fraction (Figures 19 and 20).

Differences in particulate P removal depended more on the size of the filter medium than the type (Table 9). Removal of PP at 50% or better was achieved in the medium (2.0 – 3.4 mm) and fine (0.25-0.85mm) size sands except for the iron-coated sand. Removal of DOP was negligible across all size ranges and filter media types (Table 9). DOP was released in the iron-coated sand treatment.

The Pro-Sil Plus™ media reduced calcium and alkalinity concentrations by ~5%, whereas for other media types these constituents increased or remained unchanged (Table 9). The iron-coated sand columns released large quantities of SRP once flow was initiated (Figure 21). Although the release rate decreased since startup, export continued through the last week of the study.

Table 9. Mean (± 1 s.d.) TP, SRP, PP, DOP, calcium and alkalinity concentrations in the inflow and outflows of filter media columns during the August 18-November 17, 2000 period of record.

	Inflow	Quartz			Limerock		Pro-Sil Plus™		Iron-coated Sand
		Coarse	Med.	Fine	Coarse	Med.	Coarse	Med.	Fine
Total P ($\mu\text{g/L}$)	17 \pm 4	15 \pm 5	14 \pm 4	17 \pm 5	14 \pm 4	13 \pm 6	13 \pm 4	13 \pm 3	122 \pm 74
SRP ($\mu\text{g/L}$)	3 \pm 1	4 \pm 2	4 \pm 2	7 \pm 3	3 \pm 2	3 \pm 1	3 \pm 1	2 \pm 1	87 \pm 14
PP ($\mu\text{g/L}$)	6 \pm 2	4 \pm 1	3 \pm 2	2 \pm 2	4 \pm 1	3 \pm 2	4 \pm 2	3 \pm 1	19 \pm 23
DOP ($\mu\text{g/L}$)	8 \pm 2	7 \pm 1	7 \pm 1	8 \pm 2	7 \pm 1	7 \pm 1	7 \pm 1	7 \pm 2	17 \pm 5
Calcium (mg/L)	74 \pm 5	77 \pm 6	76 \pm 6	77 \pm 5	77 \pm 5	77 \pm 5	71 \pm 12	72 \pm 12	73 \pm 7
Alkalinity (mgCaCO_3/L)	253 \pm 12	261 \pm 14	261 \pm 12	260 \pm 17	260 \pm 14	263 \pm 12	248 \pm 46	246 \pm 50	263 \pm 16

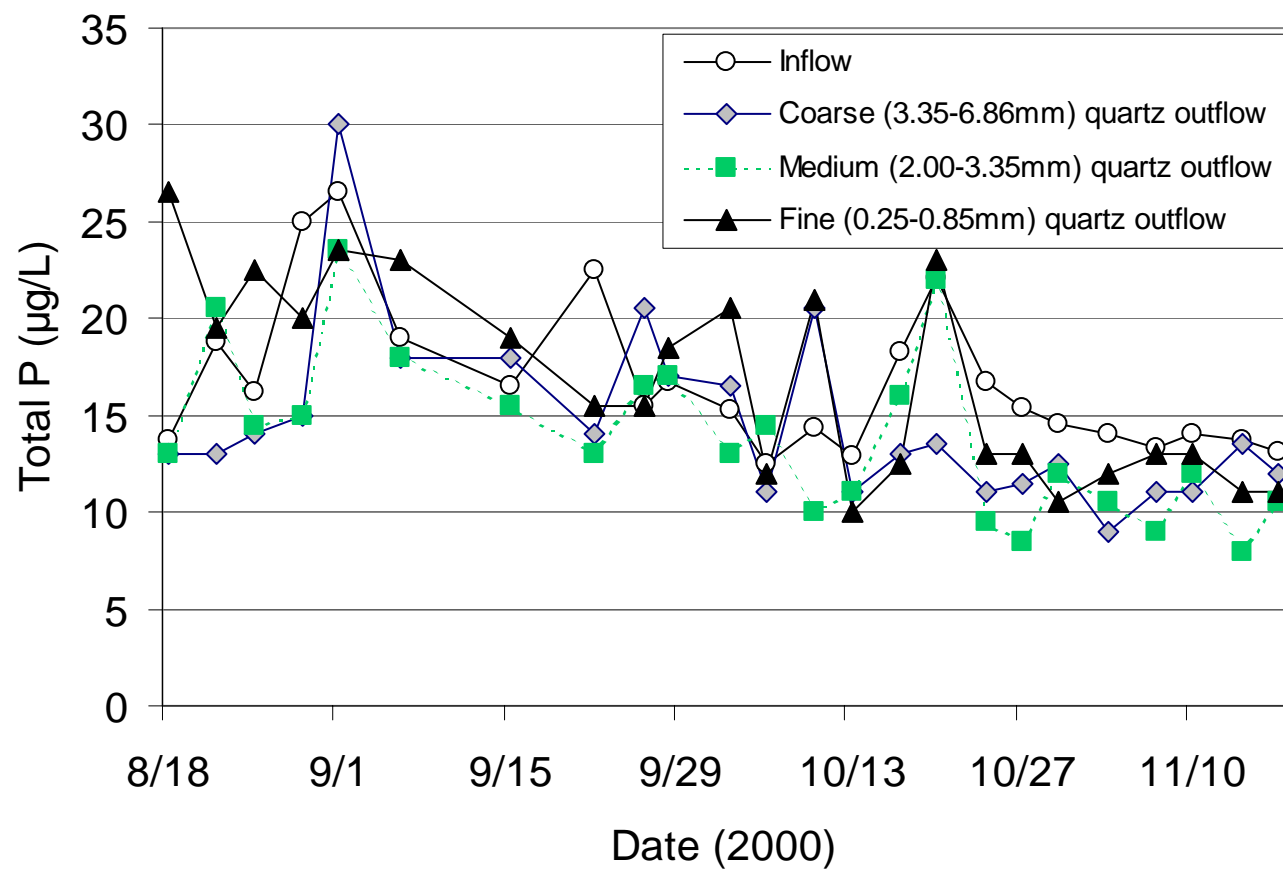


Figure 16. Mean (\pm s.d.) total phosphorus concentrations in the inflow and outflow of duplicate filter columns with each pair containing one of three size fractions of quartz “sand”. Post-STA water was fed to the columns during a three-month monitoring period.

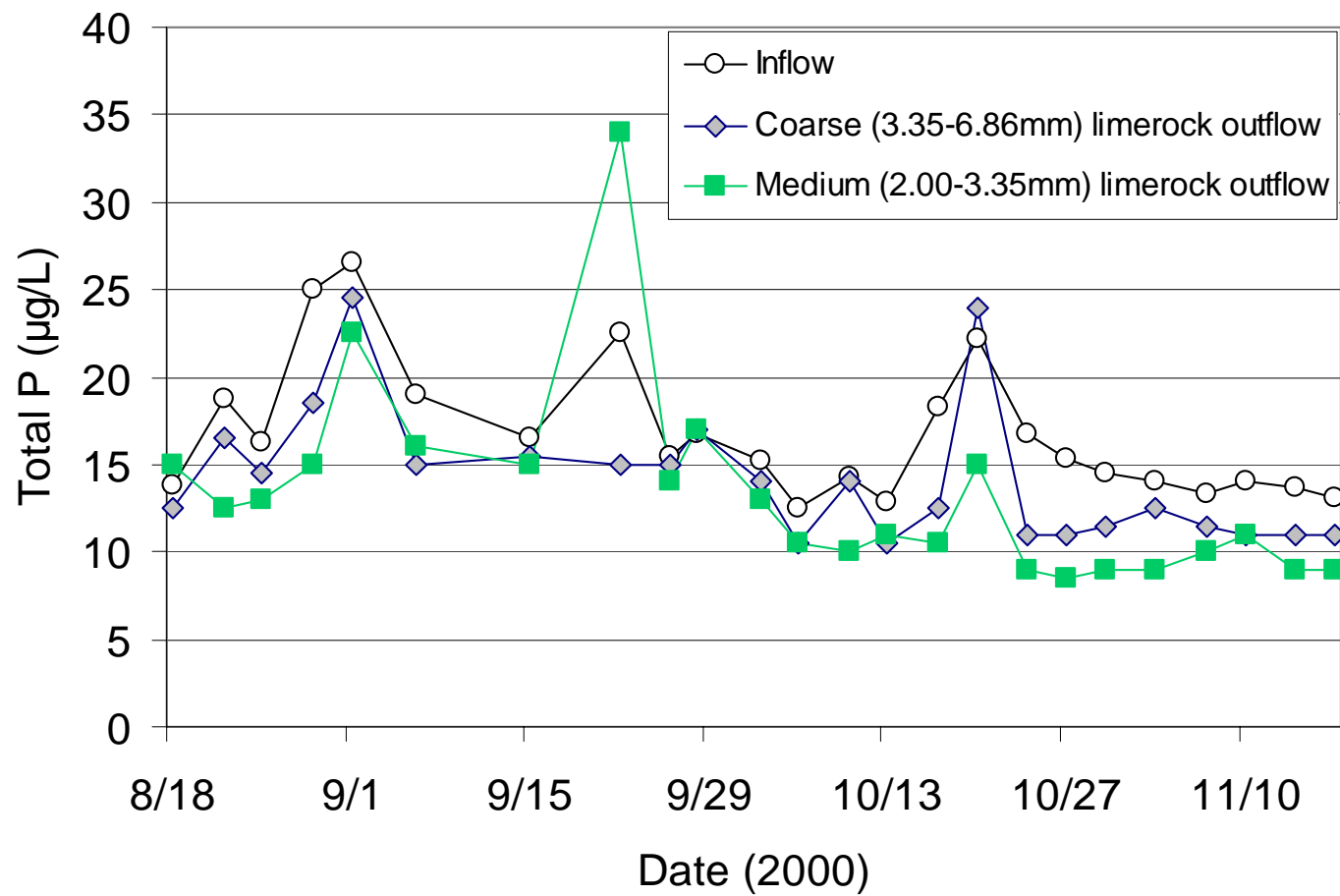


Figure 17. Mean total phosphorus concentration in the inflow and outflows of duplicate filter columns with each pair containing one of two size fractions of limerock. Post-STA water was fed to the columns during a three-month period.

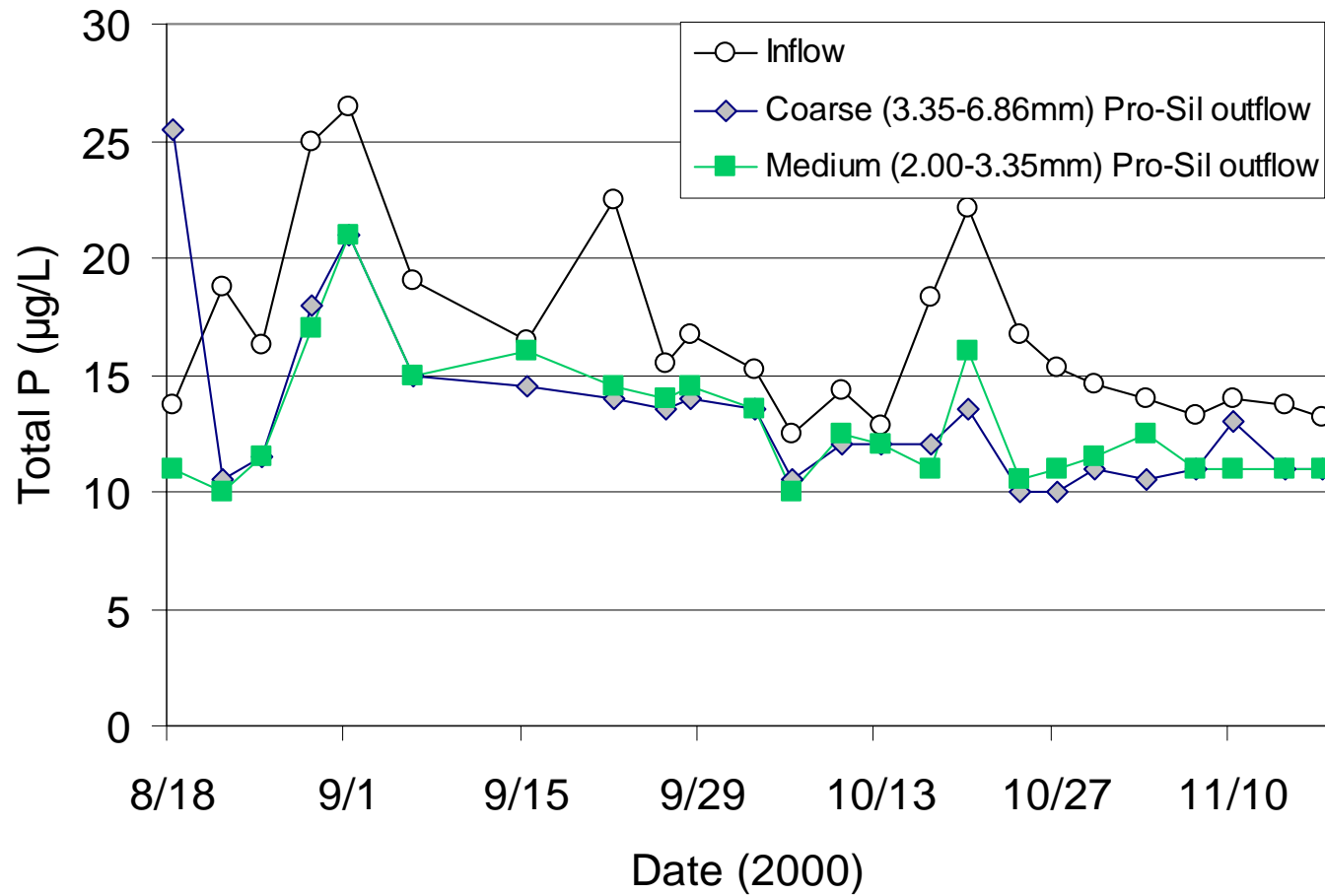


Figure 18. Mean total phosphorus concentration in the inflow and outflows of duplicate filter columns with each pair containing one of two size fractions of Pro-Sil® (Ca-Mg silicate). Post-STA water was fed to the columns during a three-month period.

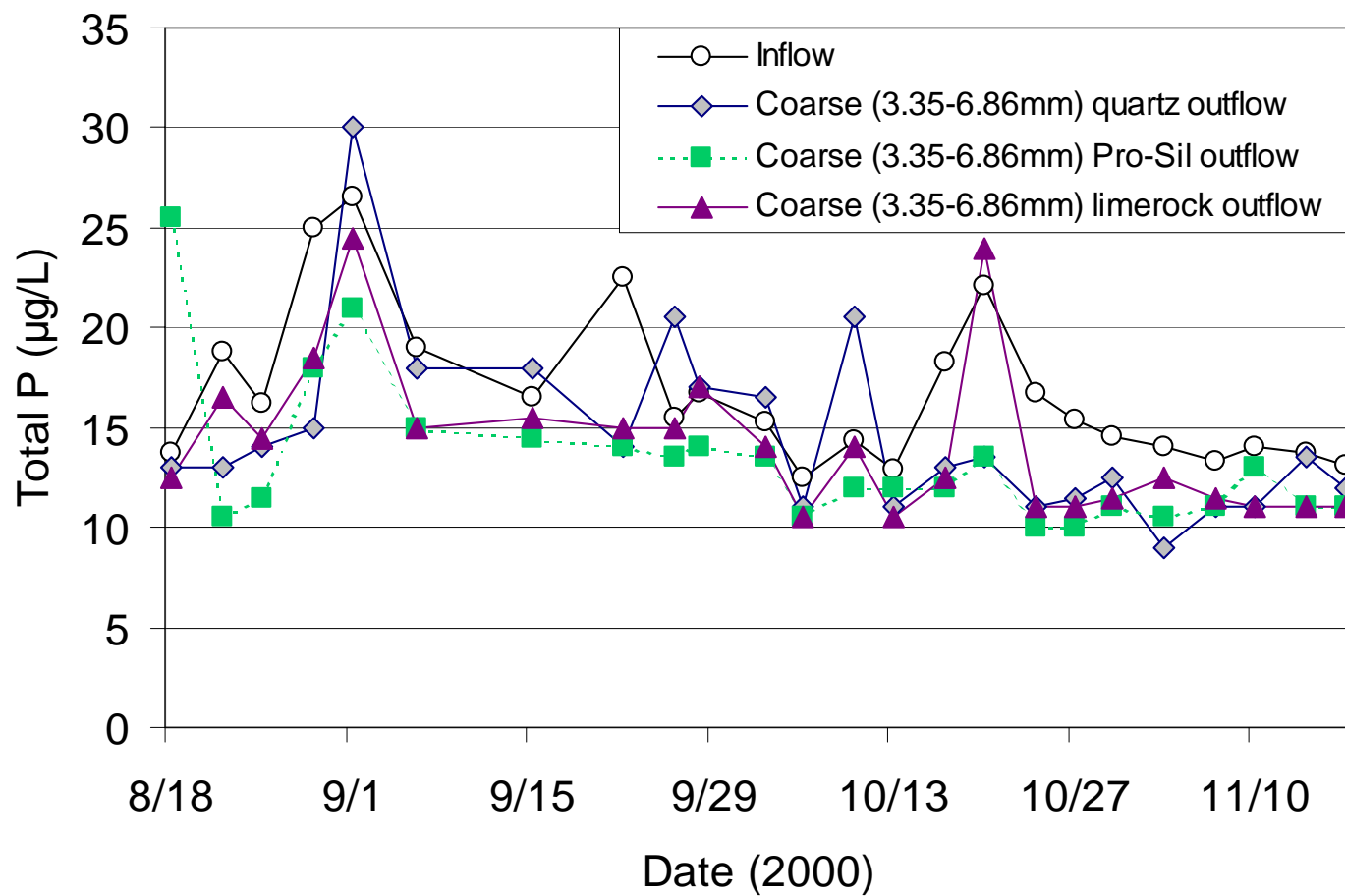


Figure 19. Mean total phosphorus concentrations in the inflow and outflows of duplicate filter columns with each pair containing a coarse grade of one of three substrate types. Post-STA water was fed to the columns during a three-month period.

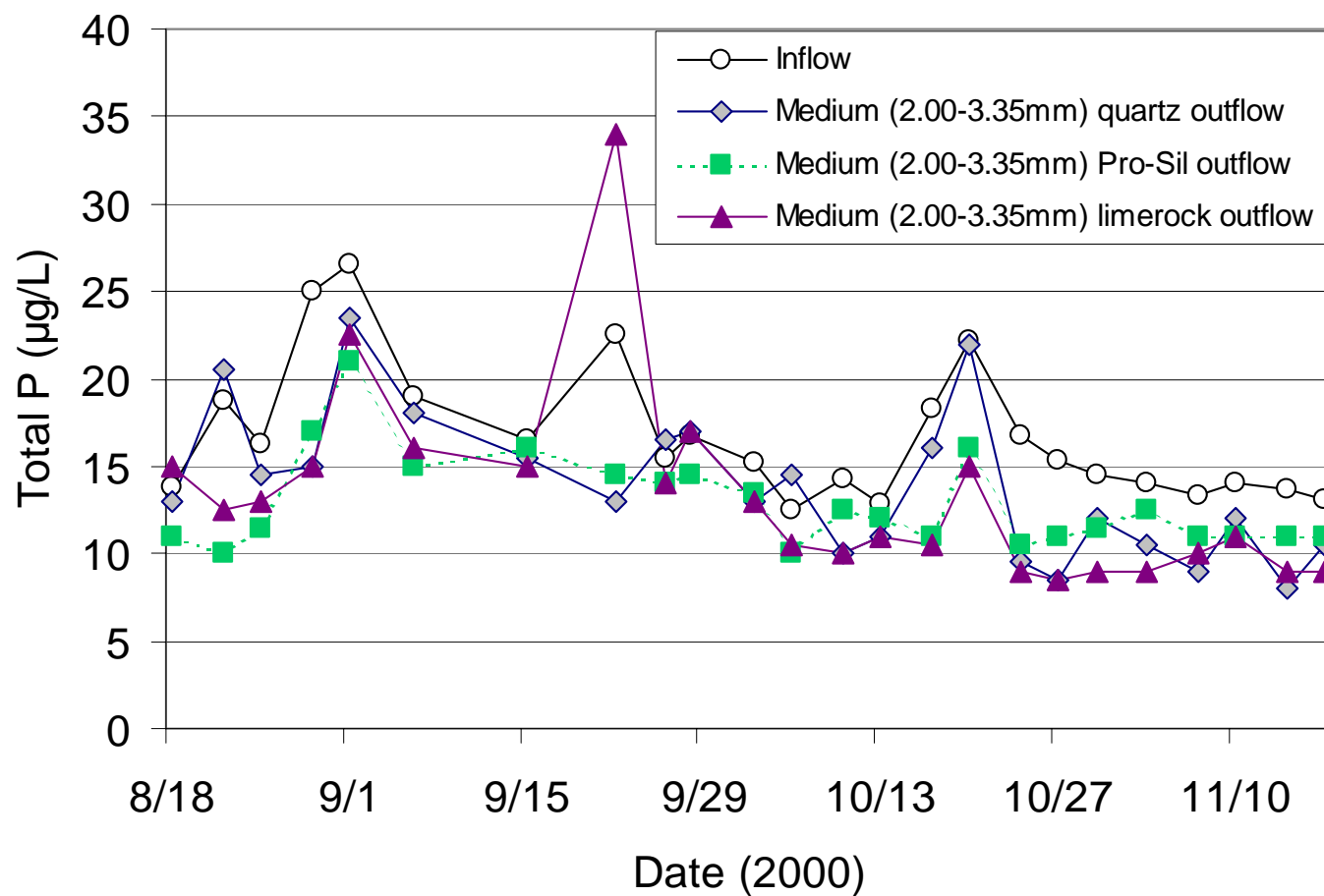


Figure 20. Mean total phosphorus concentrations in the inflow and outflows of duplicate filter columns with each pair containing a medium grade of one of three substrate types. Post-STA water was fed to the columns during a three-month period.

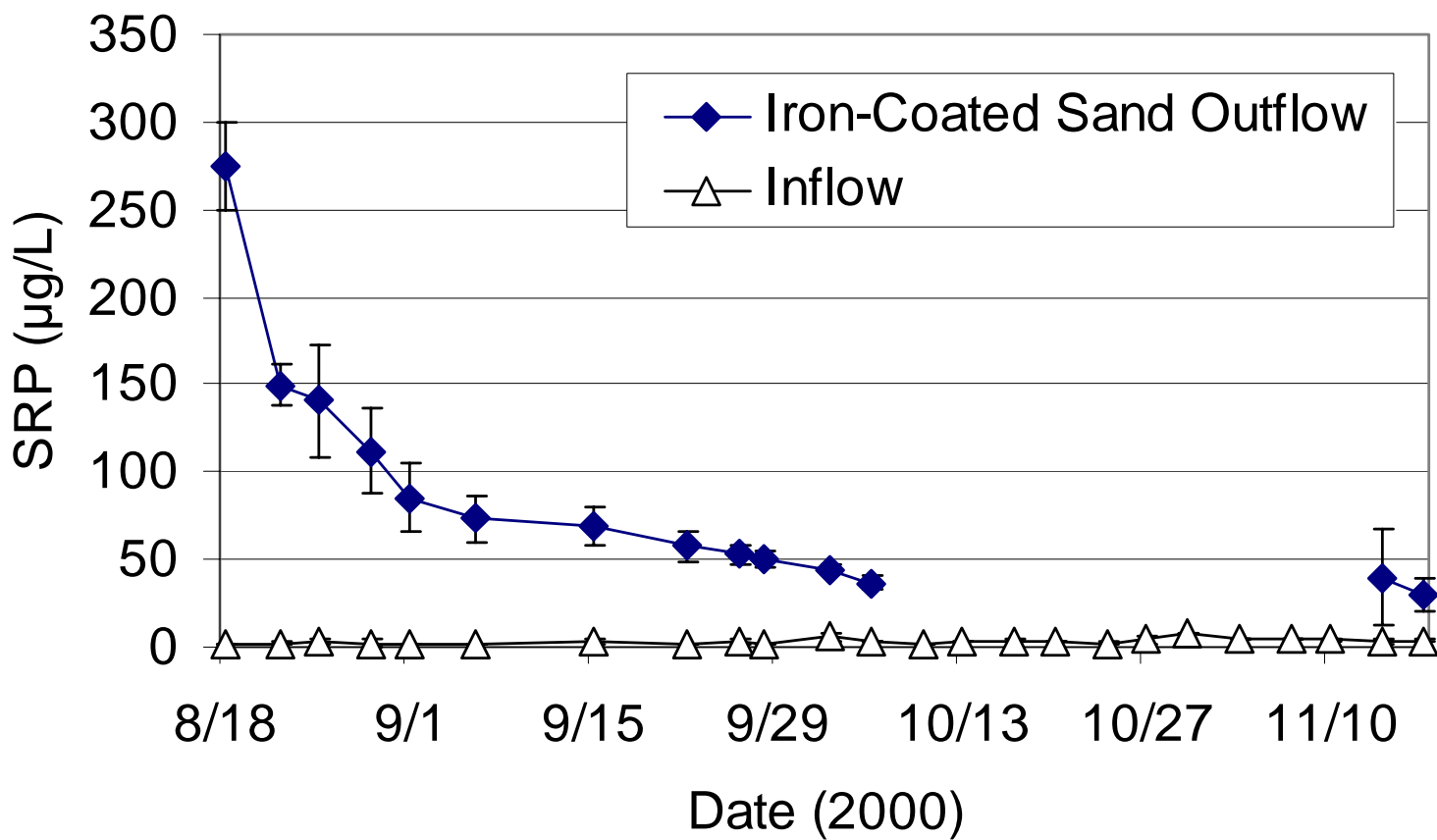


Figure 21. Mean (\pm s.d.) soluble reactive phosphorus concentrations in the inflow and outflow of duplicate iron-coated sand filter columns. Post-STA water was fed to the columns during a three-month monitoring period.

Particulate Phosphorus and Dissolved Organic Phosphorus Characterization and Stability (Subtask 5xi)

Findings from DBE's Phase I research demonstrated that the effluent from both SAV and LR unit processes consists largely of particulate P (PP) and dissolved organic P (DOP). The ability of a supplemental technology to achieve the 10 ppb TP target depends on its ability to reduce these fractions to extremely low levels. The capabilities of the supplemental technologies to "treat" these P species will vary, depending on the size fraction, stability, and transportability. It would be helpful in the design of STAs to understand whether particles exported from a SAV or cattail unit process are the same particles in the inflow source water, or if they are generated internally in the wetland. Understanding the differences, if any exist, of particle type, size and zeta potential (the potential difference between the plane of shear and the bulk phase), will provide insight on the transport potential of those particles.

Particulate Phosphorus Characterization in the Inflows and Outflows of Test Cells and Cell 4.

Introduction

Under a subcontract to Dr. Willie Harris of the Soil and Water Science Department at the University of Florida, inflow and outflow particles from two of the test cells (NTC-1 and NTC-5) and Cell 4 were characterized. The objective was to compare the inflow and outflow particles according to their particle size, surface charge, and elemental and mineral composition. Changes in these properties upon passage through wetlands dominated by SAV and cattail communities indicate how wetlands process P-associated particulates. Separation of the particles into various size fractions was performed by HSA/CRA and DBE personnel, using tangential flow filtration (TFF).

Methods:

1. Sample collection, handling, and characterization

Water from the outflow and inflow of Cell 4 of the ENR Project was sampled in 20-L red plastic containers over the period 8/2/00 - 8/3/00. Twenty-L samples were also collected at the outflows of NTC-5 (cattail treatment) and NTC-1 (SAV treatment), and at the inflow of NTC-1. The 20-L samples were used to concentrate particulates using tangential flow filtration (TFF).

Twenty-one additional samples were collected in plastic 4-L containers over the same time period for the purpose of replication at the Cell 4 inflow and outflow and at the Cell 2 outflow (which enters into Cell 4). Half (11) of the latter samples were inadvertently contaminated by traces of talc, which was revealed by x-ray diffraction, and were not included in the study. Another sampling using 4-L containers was conducted on 9/8/00. This latter sampling included 12 Cell 4 outflow samples, 6 Cell 4 inflow region samples, and 6 Cell 2 outflow samples. The source of the talc on the first sampling, a coarse screen used to remove floating debris, was eliminated on the second sampling. The same compositional trends were observed for both sampling periods, though higher concentrations of particulates and phosphorus were measured for the second sampling.

All sample containers were pre-washed with distilled de-ionized water. Containers for aliquots of samples to be used for TP, TSP, and SRP determinations were pre-washed with dilute HCl and rinsed with distilled de-ionized water. Stagnant areas near the shore or near culverts were avoided, as necessary, using an extension tube and pump. Water was pulled through flexible tubing by the pump directly into containers. The tubing and containers were rinsed twice with the water at the sampling site prior to collecting each sample. Samples were maintained under cold (ice or refrigerator) and suppressed-light conditions prior to, during, and subsequent to the filtration processing as described below.

2. Particle concentration

Particles were concentrated into a slurry using TFF, which permits the processing of large volumes of water. Samples were filtered through two cassettes, each of which was fitted with two 0.40 μm polysulfonate filters, until volume reductions of approximately 15-fold (e.g., from 15 L to about 1 L) were achieved. The system was operated at the maximum cross flow velocity and minimum trans-membrane pressure, in order to minimize buildup of particles on the filters. Nevertheless, some material was observed on the filter, and particulate concentrations were not calculated from TFF concentrates. Instead, they were determined from dead-end filtration on replicated aliquots of the water samples.

Particles in the 4-L replication samples (35 total) were collected via "dead-end" filtration, using 0.45-micrometer filters. Retentate was removed from the filters and transferred to a glass slide while still moist, using a rubber policeman. The material was scraped from the glass slide onto weighing paper after it had air-dried, and then stored in vials at 4°C in the dark until analyzed.

3. Particle size and surface charge analyses

Particle size and surface charge characteristics, which relate to dispersibility and transport potential of particles, were conducted on each sample at the University of Florida Engineering Research Center (ERC).

Particle size was determined using light scattering technology (Weiss and Frock, 1976). This is a well-established approach which exploits the relationship between particle size and the intensity, polarization, and angular distribution of light scattered from particles dispersed in a liquid medium (van de Hurst, 1981). The instrument used was the Beckman Coulter LS 230 Enhanced Laser Diffraction Analyzer (Beckman Coulter, Inc, 1950 W. 8th Ave., Hialeah, FL), which is maintained at the University of Florida Engineering Research Center. This instrument is reported to discriminate in the 0.04- 2000 µm particle size range. (The original plan of work specified that particle size analysis would be conducted using electroacoustic analysis, but preliminary assessment of the sample indicated that light scattering would be more applicable given the dilute nature of the sample suspensions being analyzed.)

Surface charge of particles was determined by electrophoretic light scattering, which entails assessment of doppler shifting in relation to a reference beam (Thompson, 1992). The instrument used is the Model "Zeta Plus" Zeta Potential Analyzer (Brookhaven Instrument Corporation, 750 Bluepoint Road, Holtsville, NY), which is maintained at the University of Florida Engineering Research Center. This instrument is reported to be suitable for particles with the size range of 0.005 to 30 µm.

4. Micro-morphological and elemental analyses

Morphology of particles was assessed using a scanning electron microscope (SEM) at the Major Analytical Instrument Cooperative (Materials Engineering Department). Secondary electron

images were obtained at various magnifications. Care was taken for the replicated samples to collect at least one image at a standard magnification for each sample. In addition, elemental spectra were generated from individual particles and from masses of particles using energy-dispersive x-ray fluorescence analysis, which is an accessory capability of the SEM instrumentation. Elemental spectra of selected thermogravimetry (TG) residues were also obtained in order to confirm that silicon, calcium, and oxygen comprised the bulk of the residues. Elemental dot maps relating concentrations of P, Si, Ca, S, Cl and Fe to discrete particles within the field of view of the image were generated.

5. Mineralogical analysis

Mineralogical analyses were conducted at the Soil Mineralogy Laboratory (Soil and Water Science Department). Bulk mineralogy of the suspended material was determined by x-ray diffraction (Whittig and Allardice, 1986) and thermal analysis (Karathanasis and Harris, 1994). Mineralogy was determined on the residue after selective dissolution of carbonates and organic matter, and on magnetic separates collected using the High Gradient Magnetic Separation (HGMS) system. The intent was to evaluate the possibility that discrete calcium phosphate or iron phosphate phases are forming, as opposed to sorption of phosphate on calcium carbonate.

a. X-ray diffraction

Crystalline components in samples were analyzed by x-ray powder diffraction (Whittig and Allardice, 1986). Samples were mounted as a powder on specially cut quartz crystals that minimize background x-ray scattering (noise). Samples were scanned from 2 to 40 degrees 2 (or higher if necessary) under Cu K α radiation, using a computer-controlled x-ray diffractometer equipped with stepping motor and graphite crystal monochromator. Minerals were identified from diffraction peaks using reference diffraction data of minerals compiled by the International Center for Diffraction Data (1601 Park, Lane, Swarthmore, PA 19801) (Bayliss et al., 1980).

b. Thermal analysis

Solids were analyzed by thermogravimetry (TG), which is a technique in which the mass of a substance is monitored as a function of temperature or time as the sample is subjected to a

controlled temperature program (Earnest, 1988). Mass loss or gain as the sample is heated can be used diagnostically to corroborate the presence of solid phases present in the sample, and in some cases (e.g., calcite) to quantify a phase based on the stoichiometry of the reaction (Karathanasis and Harris, 1994). The TG analyses were conducted using a computer controlled thermal analysis system, which collects and stores data digitally and permits computer calculations of reaction weight losses. The percentage of organic matter was estimated to be the loss upon ignition. Calcium carbonate content was calculated based upon CO₂ evolution that began between 670-700 °C. 'Silica' content was calculated by subtracting the weight of CaO in the TG residue from the total residue weight.

6. Chemical analysis

Characterization on aliquots of each sample prior to and following TFF concentration included pH, electrical conductivity (EC), total solids, total P (TP), total soluble phosphorus (TSP), soluble reactive P (SRP), total C (TC), and inorganic C (IC). Phosphorus analyses for the TFF samples were performed by DB Environmental (DBE); P analyses for the replicated samples were performed both by DBE and UF in August, and exclusively by UF in September. There were three replicates per location in the sampling scheme. Determinations of pH and EC were made using standard laboratory meters. Descriptions of other chemical methods are given below.

a. Total solids

Methods used to determine total and suspended solids deviated from U.S. E.P.A. method 160.1-160.2 because solids in water samples were significantly lower than the practical range of determination for these methods. Total solids determinations were performed in triplicate. Five-ml aliquots of homogenized water samples were pipeted into desiccated pre-weighed aluminum weighing dishes. Samples were dried at 40 °C and placed in a desiccator for approximately 48 hours. The weighing dishes were then re-weighed, and total solids were quantified via subtraction. For suspended solids determinations, 450 ml aliquots of homogenized water samples were filtered through pre-washed 0.40 µm filters. Material retained by the filter was then washed with three 15-ml aliquots of distilled de-ionized water. Filters were dried at 40 °C and placed in a desiccator for approximately 48 hours. Filters were

then re-hydrated with distilled de-ionized water. Material was removed and allowed to dry under laboratory conditions. Removal of material from filters was performed on two consecutive days, and the relative humidity as measured by a 'relative humidity meter' was stable over this period.

b. TP and TSP

Aliquots of water samples used for TSP determinations were filtered using 0.45 µm PES syringe filters within 6 hours of sample collection. Both TP and TSP samples were preserved with H₂SO₄ and iced on 8/2-8/3. Samples were refrigerated until digested. Samples were digested in an autoclave on 8/9 and quantified colorimetrically according to U.S. E.P.A. (1979) Method 365.2. PP was calculated by subtraction (TP- TSP = PP). QA/QC protocols followed included the digestion of replicate samples and matrix spikes as well as an external organic P standard.

c. SRP

Aliquots of water samples used for SRP determinations were filtered and immediately iced. Samples were kept at approximately 4 C prior to determination. SRP was quantified on 8/7 according to EPA (1979) Method 365.2.

d. TC and IC

TC and IC of the TFF filtrate and retentate, and the filtrate and raw water of the replicated samples, were determined on 8/11 and 8/19 using a total carbon analyzer. Samples used for C determinations were refrigerated and kept dark prior to analysis. TC and IC analyses were based upon the pyrolysis of C compounds and the analysis of liberated CO₂ by infrared spectrophotometry. QA/QC protocols followed included the analysis of replicate samples and matrix spikes. TOC was calculated by subtraction (TC-IC= TOC).

Results and Discussion

1. North Test Cells

Calcite was present in the inflow water to NTC-1 (dominated by SAV) and the outflow waters from NTC-1 and the cattail dominated NTC-5 (Figure 22). Kaolinite was present in the NTC-1 outflow particulates, which may have been caused by a resuspension of the bottom muck layers

by a population of small alligators. The absence of prominent peaks suggest that most of this material is noncrystalline. Elemental spectra (EDX) indicate higher S in the particles in NTC-5 outflow compared to either the inflow or outflow of NTC-1. NTC-1 outflow has higher aluminum than any other sample, which is consistent with the presence of kaolinite detected by XRD. Results of thermal gravimetric (TG) analysis show that organic matter is the most abundant particulate matter in all the samples (see Figure 23 for an example of a TG weight loss curve for particles collected from Cell 4).

2. Cell 4

The dominant suspended particulate components in ENR Cell 4 water samples were organic matter, silica, and calcium carbonate (Figure 23). Although calcite was present in all samples, it was most abundant in Cell 4 outflow particulates (Figure 22). Algae (including diatoms) appear to comprise a substantial portion of the sample, based on optical and SEM observations (Figure 24). Most of the silica was probably derived from diatoms (Figure 25). This study did not involve a quantitative assessment of algae, or the relative contributions among algae, bacteria, fungi, and detritus to the organic matter pool. SEM analyses (Figure 25) support a direct association between suspended solids and particulate P, and between particulate organic matter and particulate P (Figure 26), but an association between CaCO_3 and particulate P did not exist (Figure 27).

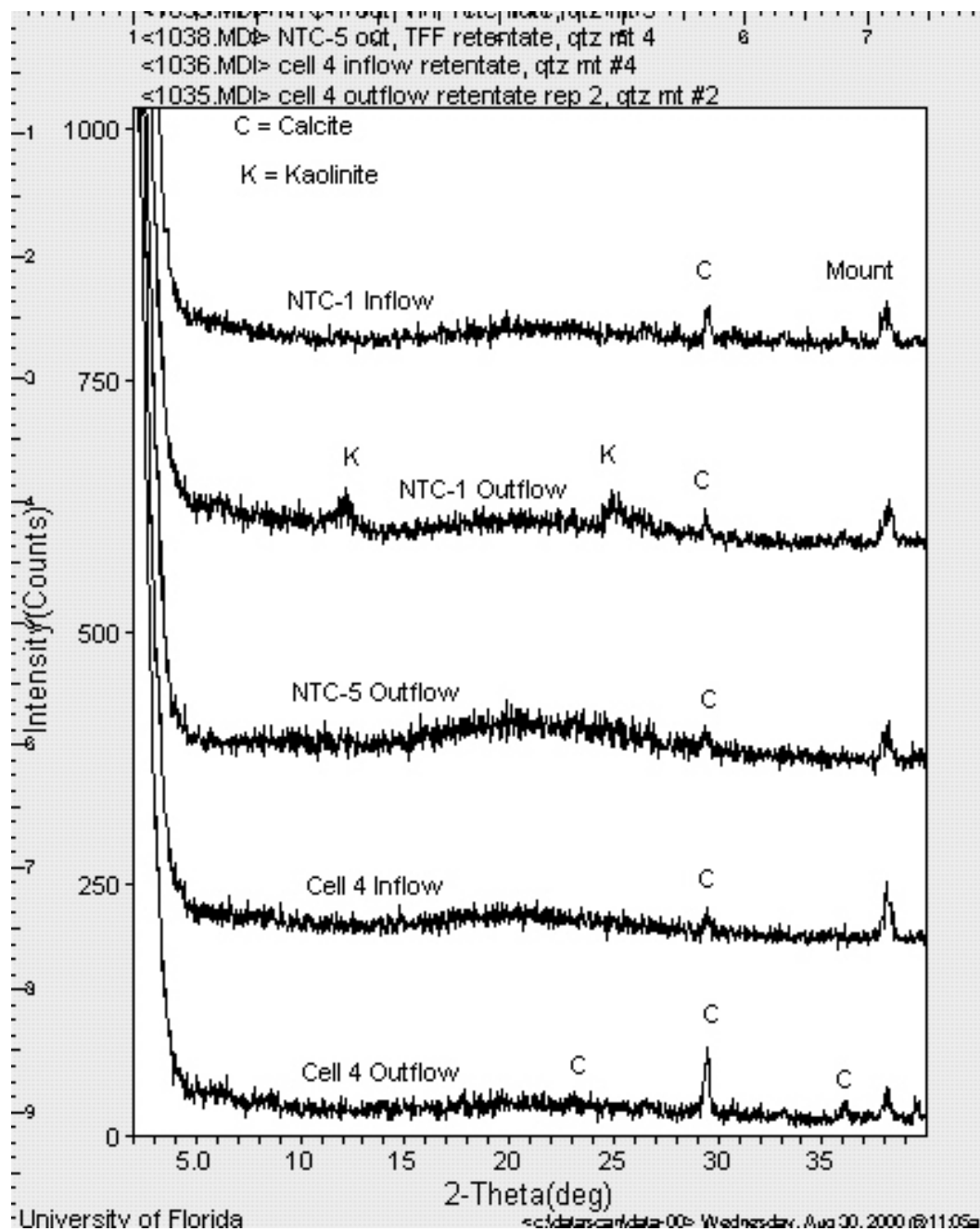


Figure 22. X-ray diffraction (XRD) patterns of TFF-concentrated particulates from Cell 4 and test cells.

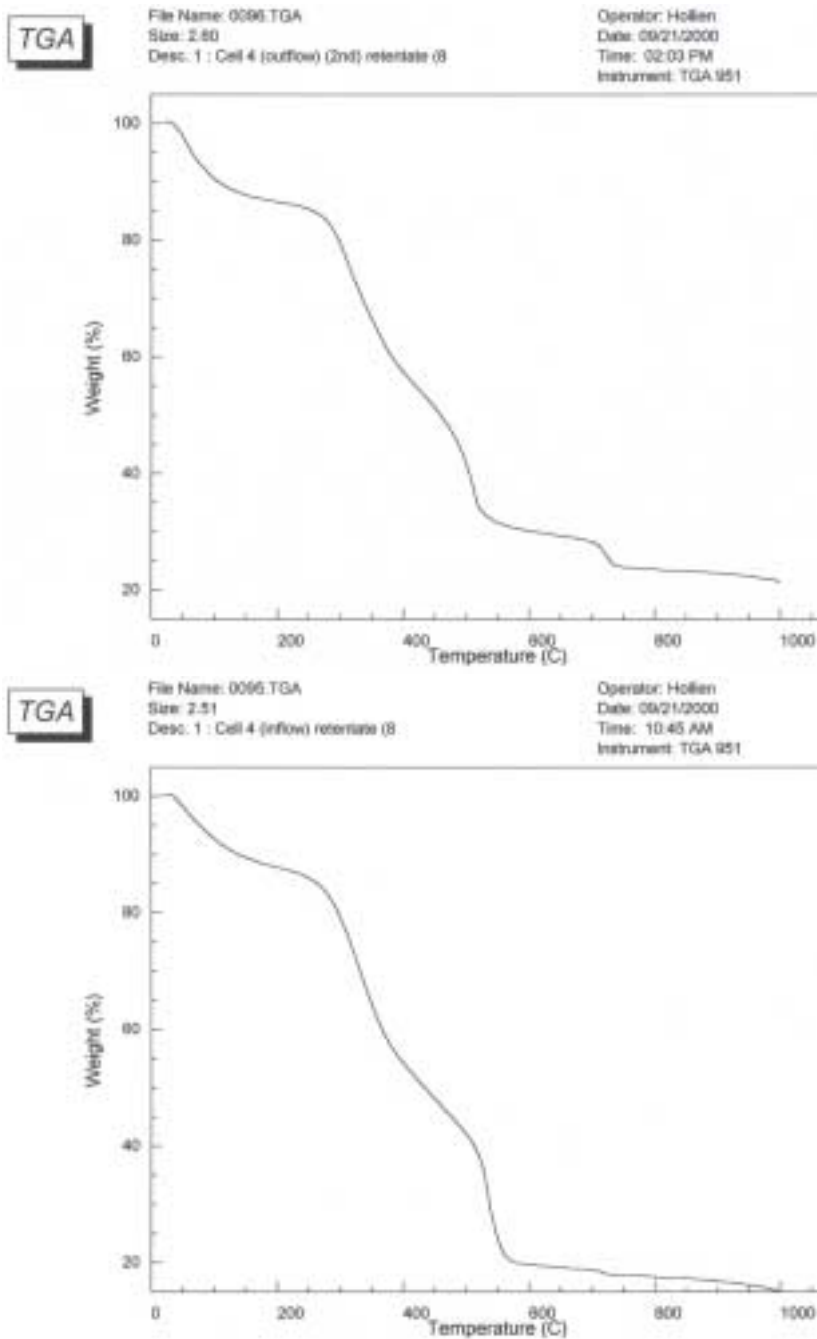


Figure 23. Thermal gravimetric weight loss curves for particulates collected from Cell 4 outflow (top) and inflow region (bottom), shown as examples. Weight loss in the range of about 325 to 550° C is attributed to organic matter combustion (CO_2 “loss on ignition”), and in the range of about 700-750° C, to conversion of calcite (CaCO_3) to CaO (CO_2 loss).

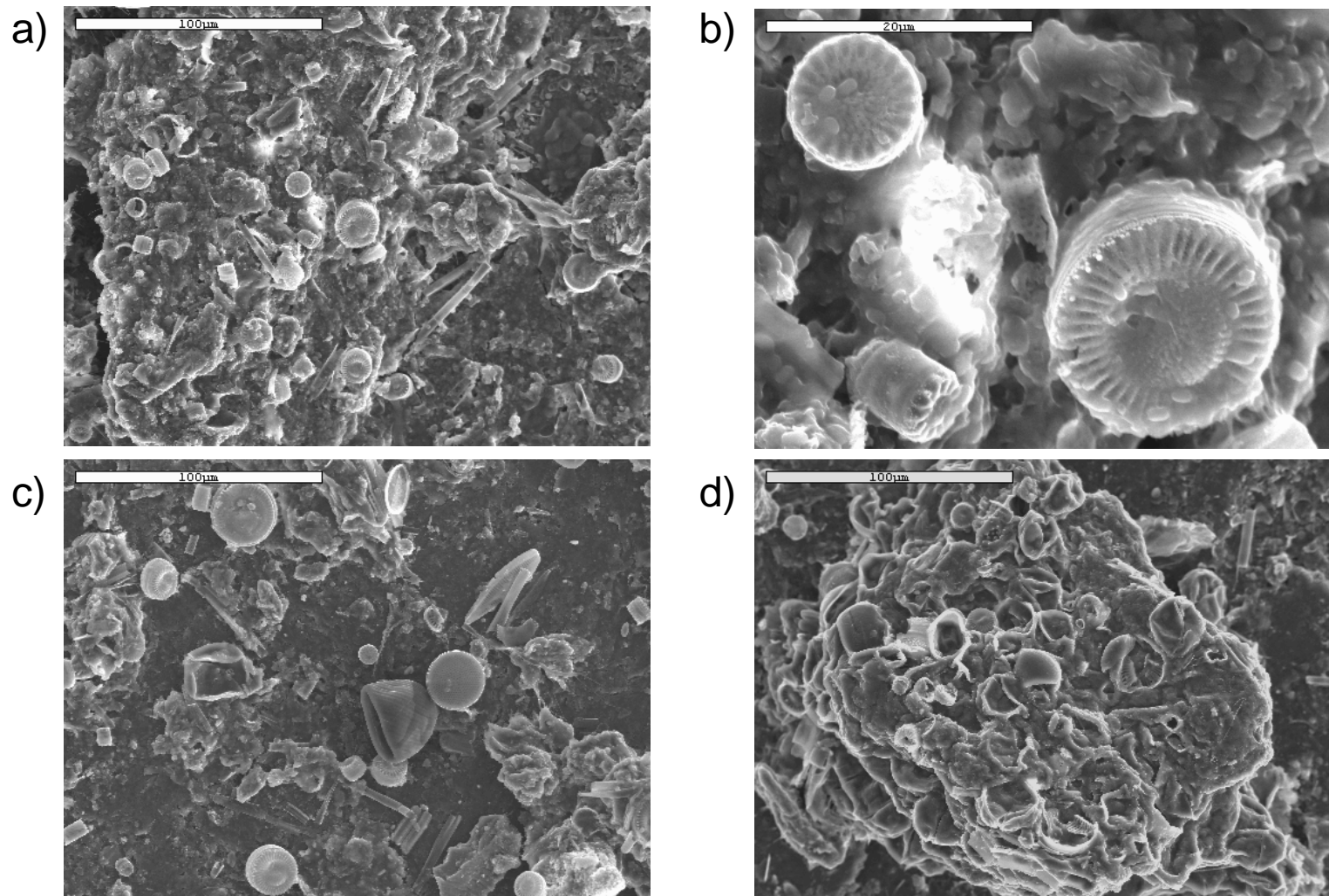


Figure 24. Algal abundance illustrated in four-image composite of SEM micrographs (clockwise from upper left) a) centric diatoms present in suspended solids from Cell 2 outflow in the September sample magnified 500x; b) diatoms from “a)” magnified 2700x; c) C-based algal ‘cells’ from Cell 2 outflow in the August sample; d) C- based cells and both centric and pinnate diatoms present in Cell 4 inflow region during September.

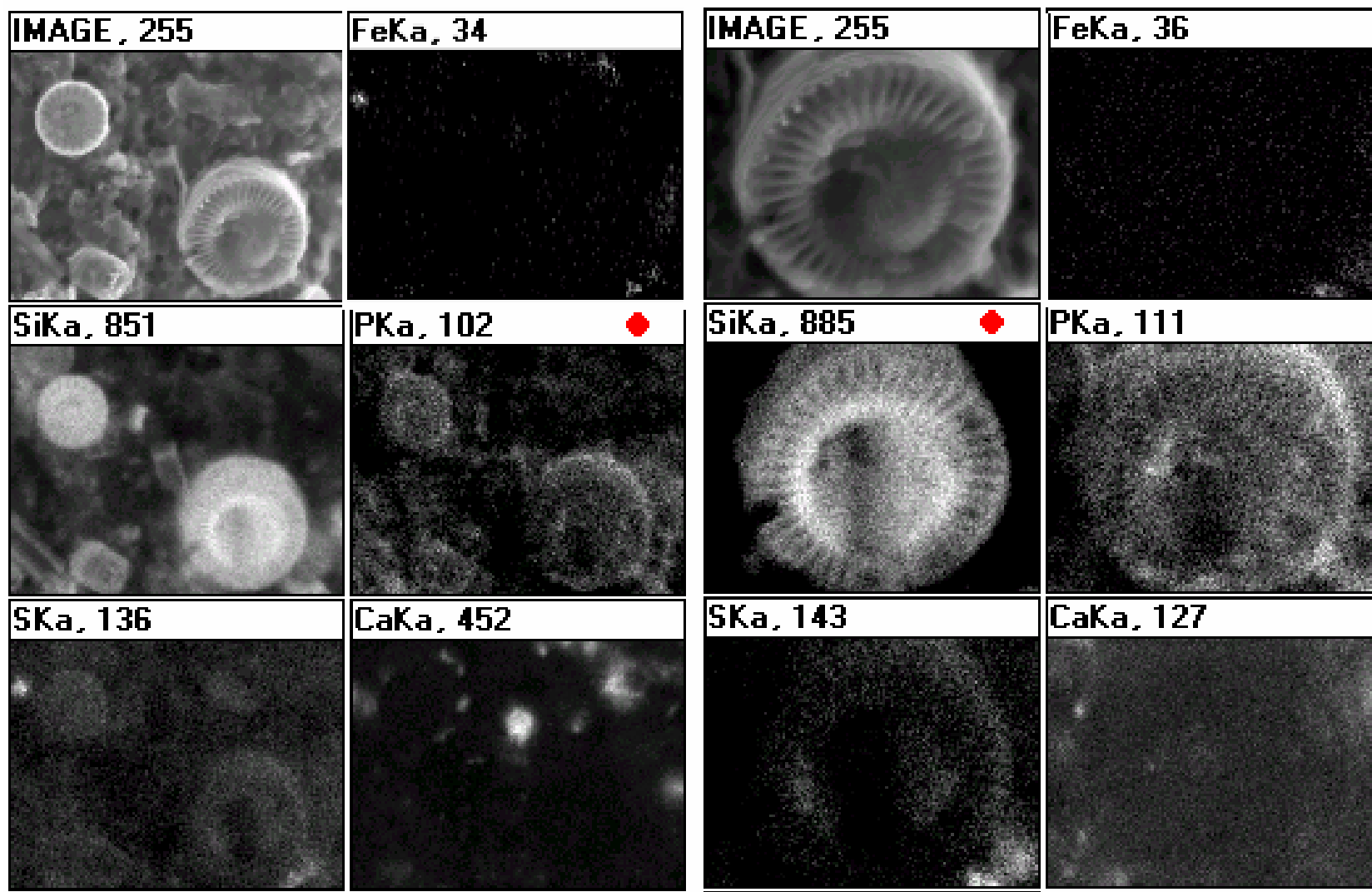


Figure 25. Two six-image composites of SEM micrographs. a) Left composite: At upper left is the same secondary electron image shown in Figure 24b. Other images are elemental dot maps of Fe, Si, P, S, and Ca, showing an association of Si and P with diatoms. b) Right composite: At upper left is a higher magnification image of the largest diatom shown in the right composite. This composite illustrates that whereas both Si and P are both associated with the diatom, they don't show strong spatial association with each other within the diatom.

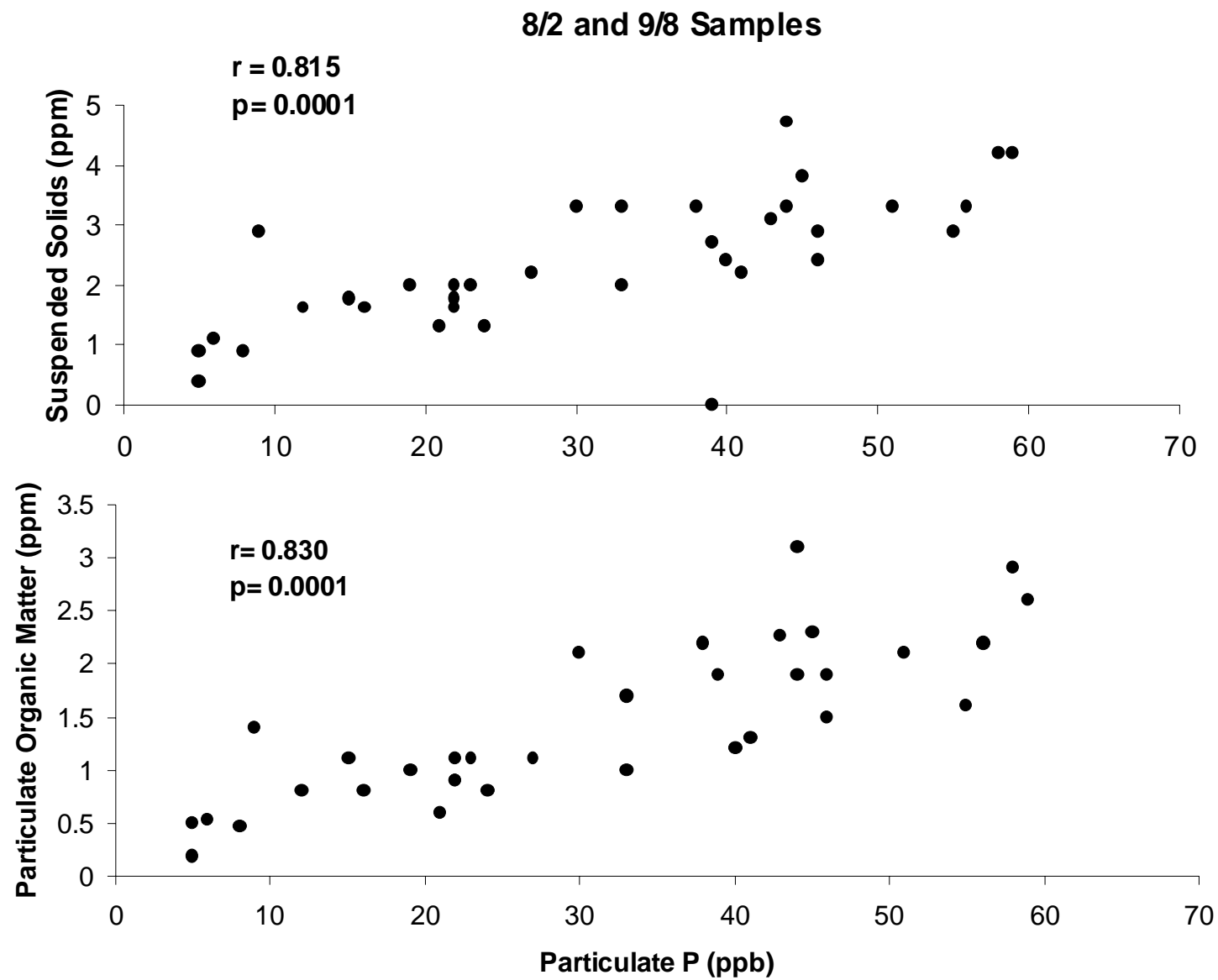


Figure 26. Scatter plots of particulate P with particulate organic matter and suspended solids.

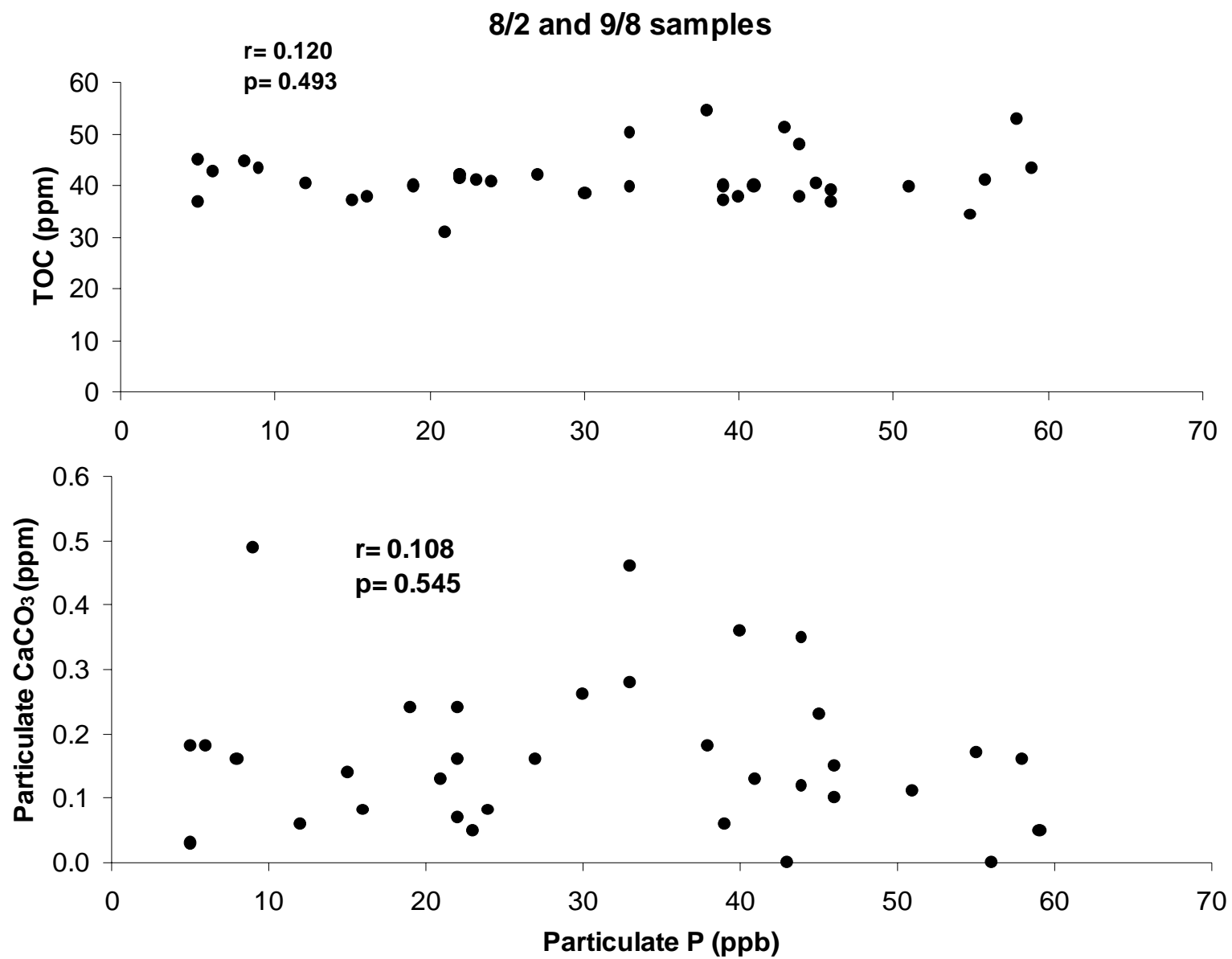


Figure 27. Scatter plots of particulate P with particulate CaCO_3 and particulate organic matter.

References

- Bayliss, P., D.K. Smith, M.E. Morse, and L.G. Berry. 1980. Mineral powder diffraction file data book. International Center for Diffraction Data, Swarthmore, PA.
- Danen-Louwerse, H.J., J.Lijklema, and M. Coenraats. 1995. Coprecipitation of phosphate with calcium carbonate in Lake Veluwe. *Water Res.* **29**: 1781 - 1785.
- DB Environmental (DBE). 2000. A Demonstration of Submerged Aquatic Vegetation/Limerock Treatment System Technology for Removing Phosphorus from Everglades Agricultural Area Waters: Follow-on Study. Third Quarterly report submitted to South Florida Water Management District and the Florida Department of Environmental Protection. West Palm Beach, FL.
- DB Environmental (DBE). 2001. A Demonstration of Submerged Aquatic Vegetation/Limerock Treatment System Technology for Removing Phosphorus from Everglades Agricultural Area Waters: Follow-on Study. Fourth Quarterly report submitted to South Florida Water Management District and the Florida Department of Environmental Protection. West Palm Beach, FL.
- Earnest, C.M. 1988. Compositional analysis by thermogravimetry. ASTM, Philadelphia, PA.
- Grossman, R.B., and J.L. Millet. 1961. Carbonate removal from soils by a modification of the acetate buffer method. *Soil Sci. Soc. Am. Proc.* 25:325-326.
- Karathanasis, A.A., and W.G. Harris. 1994. Quantitative thermal analysis of soil minerals. p. 360-411. In J. Ammonette and L.W. Zelazny (ed.) Quantitative methods in soil mineralogy. *Soil Sci. Soc. Am. Miscellaneous Publication*. Soil Sci. Soc. Am. Madison, WI.
- Lavkulich, L.M., and J.H. Wiens. 1970. Comparison of organic matter destruction by hydrogen peroxide and sodium hypochlorite and its effects on selected minerals constituents. *Soil Sci. Soc. Am. Proc.* 34:755-758.
- Murphy, T.P., K.J. Hall, and I. Yesaki. 1983. Coprecipitation of phosphate with calcite in a naturally eutrophic lake. *Limnol.Oceanogr.* **28**: 59 - 69.
- Thompson R.G. 1992. Practical zeta potential determination using electrophoretic light scattering. *Amer.Lab.* 8: 48-53.
- Seuss, E. 1970. Interaction of 5 organic compounds with calcium carbonate. 1. Association phenomena and geochemical implications. *Geochim. Cosmochim. Acta* **34**: 157 - 168.

United States Environmental Protection Agency (EPA). 1979. Methods for the Chemical Analysis of Water and Wastes. EPA-600/4-79-020. Washington, D.C.

Whittig, L.D. and W.R. Allardice. 1986. X-Ray diffraction techniques. P. 331-362 In A. Klute (ed.) Methods of soil analysis, Part 1. American Society of Agronomy. Madison, WI.

van de Hurst, H.C. 1981. Light scattering by small particles. Dover Publications, NY.

Weiss, E.L., and N.H. Frock. 1976. Rapid analysis of particle size distribution using laser light scattering. Powder Technol. 14:287-293.

Task 6. Test Cell Investigations

Inflow TP concentrations at the North Test Cell (NTC) site have been decreasing since October, 2000 (Figure 28). Average inflow TP was 82 ± 34 $\mu\text{g/L}$ during 2000, while in the November-January quarter, inflow concentrations averaged 39 ± 2 $\mu\text{g TP/L}$. Both NTC-1 and NTC-15 have provided consistent and similar outflow TP concentrations (10-20 $\mu\text{g/L}$) this quarter, and aided by the lower inflow TP concentrations this quarter, have recently reduced TP concentrations to below 10 $\mu\text{g/L}$ (Figure 28).

South Test Cell (STC)-4 exported P during the quarter (Figure 29), with concentrations increasing from 17 to 22 $\mu\text{g TP/L}$ through the cell. STC-9 performed modestly, with average inflow and outflow concentrations of 17 and 14 $\mu\text{g TP/L}$ during the same period. Improved performance by STC-9 may be attributed to the limerock berm. Outflow concentrations of SRP in both cells were near 2 $\mu\text{g/L}$ (MDL), but STC-4 outflow concentrations of DOP and PP were higher than in the STC-9 outflow. This suggests that even at low inflow TP concentrations (<20 $\mu\text{g/L}$), internally-generated dissolved and particulate organic P may necessitate a limerock filter to produce an improved outflow water quality.

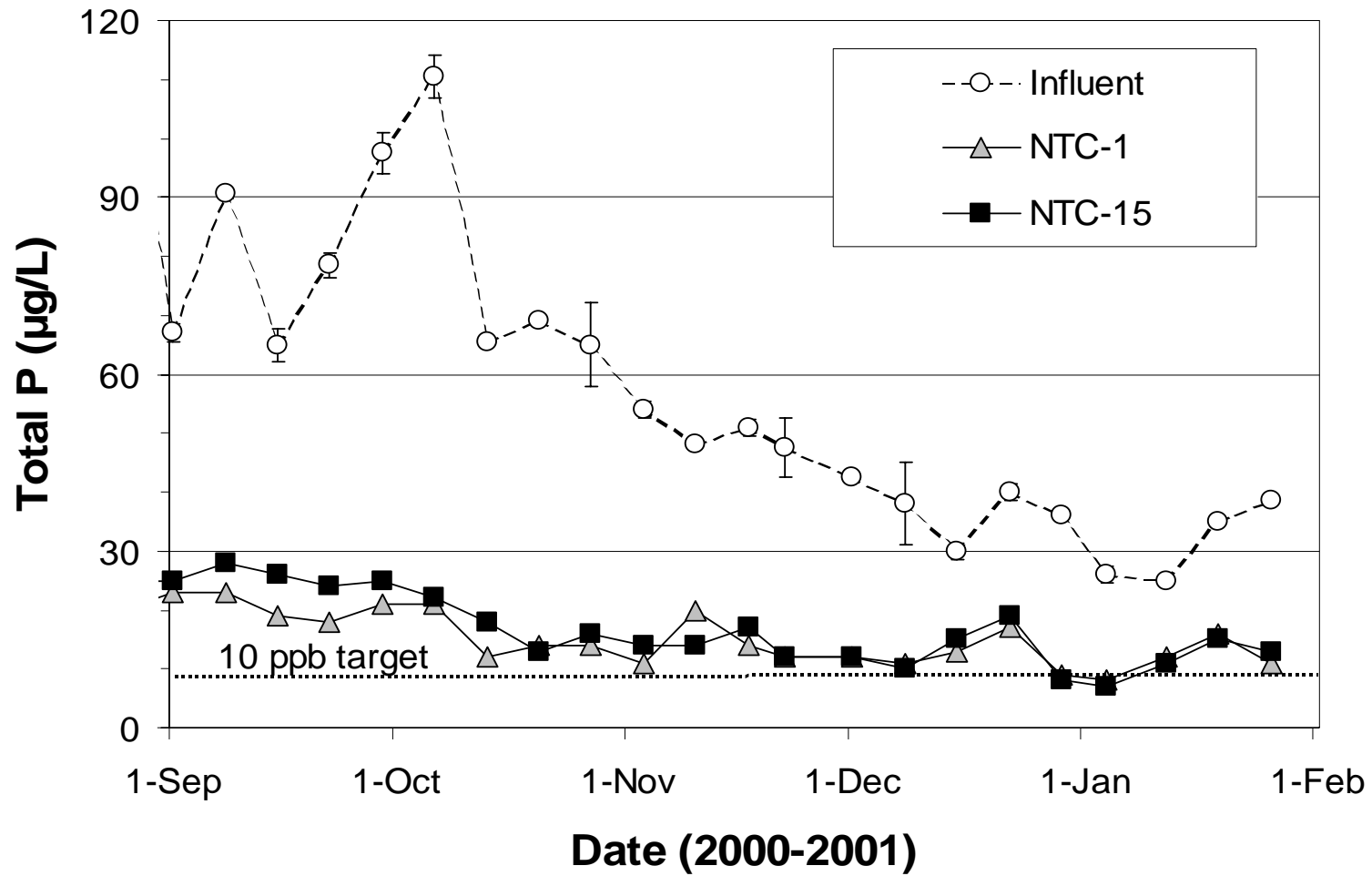


Figure 28. Total phosphorus concentrations in the inflows and outflows from north test cells NTC-1 and NTC-15. Inflow values represent the mean \pm 1 standard deviation (n=2).

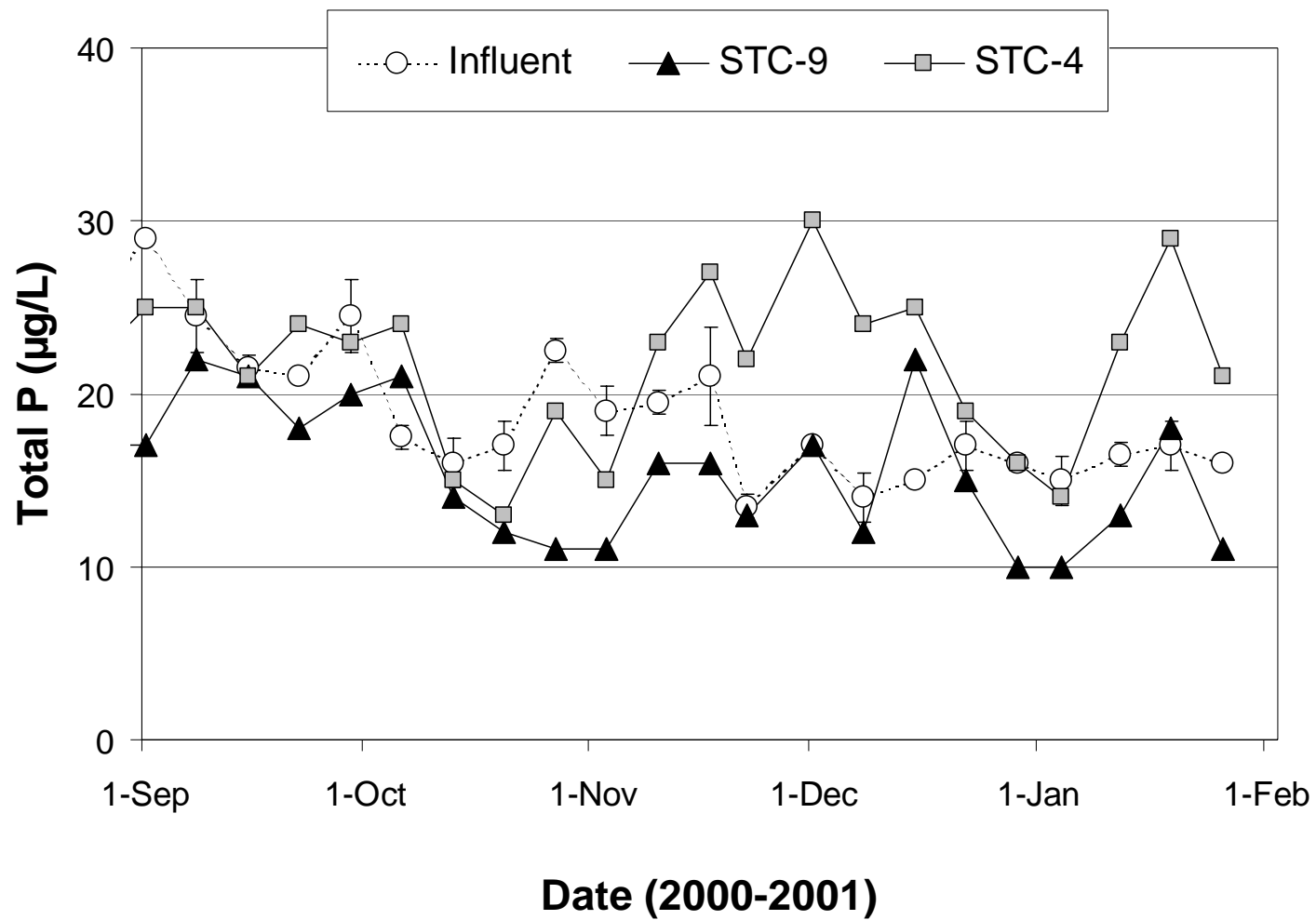


Figure 29. Total phosphorus concentrations in the inflows and outflows from south test cells STC-4 and STC-9. Inflow values represent the mean ± 1 standard deviation ($n=2$).

Task 9. Cell 4 Performance Monitoring

Construction of the L-7 east-west flow path and the inflow distribution apron, coupled with high flow 'pump-test' events have altered the hydraulics of Cell 4. On December 19, 2000, we performed an intensive sampling effort in Cell 4, similar to the August survey described in the 4th quarterly report (DBE 2001), to investigate the impact of the recent modifications on P removal performance.

During the week of the survey, inflow and outflow samples were composited from 5 weekday grabs. Cell 4 inflow contained 109 and 59 $\mu\text{g/L}$ of TP and SRP, respectively. Outflow concentrations were 45 and 18 $\mu\text{g/L}$ of TP and SRP, respectively. Alkalinity increased slightly through Cell 4, rising from 268 to 296 $\text{mg CaCO}_3/\text{L}$. A detailed analysis of the internal concentration gradients and likely short-circuit pathways of Cell 4 will be provided in the next quarterly report.

References

DB Environmental (DBE). 2001. A Demonstration of Submerged Aquatic Vegetation/Limerock Treatment System Technology for Removing Phosphorus from Everglades Agricultural Area Waters: Follow-on Study. Fourth Quarterly report submitted to South Florida Water Management District and the Florida Department of Environmental Protection. West Palm Beach, FL.

Task 10. Cell 5 SAV Inoculation and Monitoring

On November 30, we performed our fourth quarterly intensive sampling effort in Cell 5, characterizing both water quality and vegetation. *Najas guadalupensis* and *Ceratophyllum demersum* were the most prevalent species observed throughout the cell (Figures 30 and 31), while *Hydrilla sp.* was present at approximately half of the stations on the last survey (November 30, 2000) (Figure 32).

Although we observed wide variability in the SAV standing crop among stations, lowest water column SRP concentrations were generally found at the sites with greatest standing crop biomass (Figure 33). The average SAV biomass within our 24-station sampling network decreased since August (from 122 in Aug. to 90 g dry weight/m² in Nov.), even though SAV coverage appeared greater during the 120-station visual survey in November compared to a similar survey in August (Figures 30 – 32).

Cell 5 outflow-region TP concentrations have been monitored by DBE since June 2000. Concentrations have exceeded 50 µg TP/L only twice during the November-January quarter, and have averaged 36 µg/L (Figure 34). Apparent color concentrations have remained stable since October, exhibiting a range of 211 – 237 CPU and a mean of 224 CPU. SAV has continued to colonize throughout the wetland, as shown in the November Cell 5 survey (Figures 30 - 32), a factor which likely is contributing to the improved water quality.

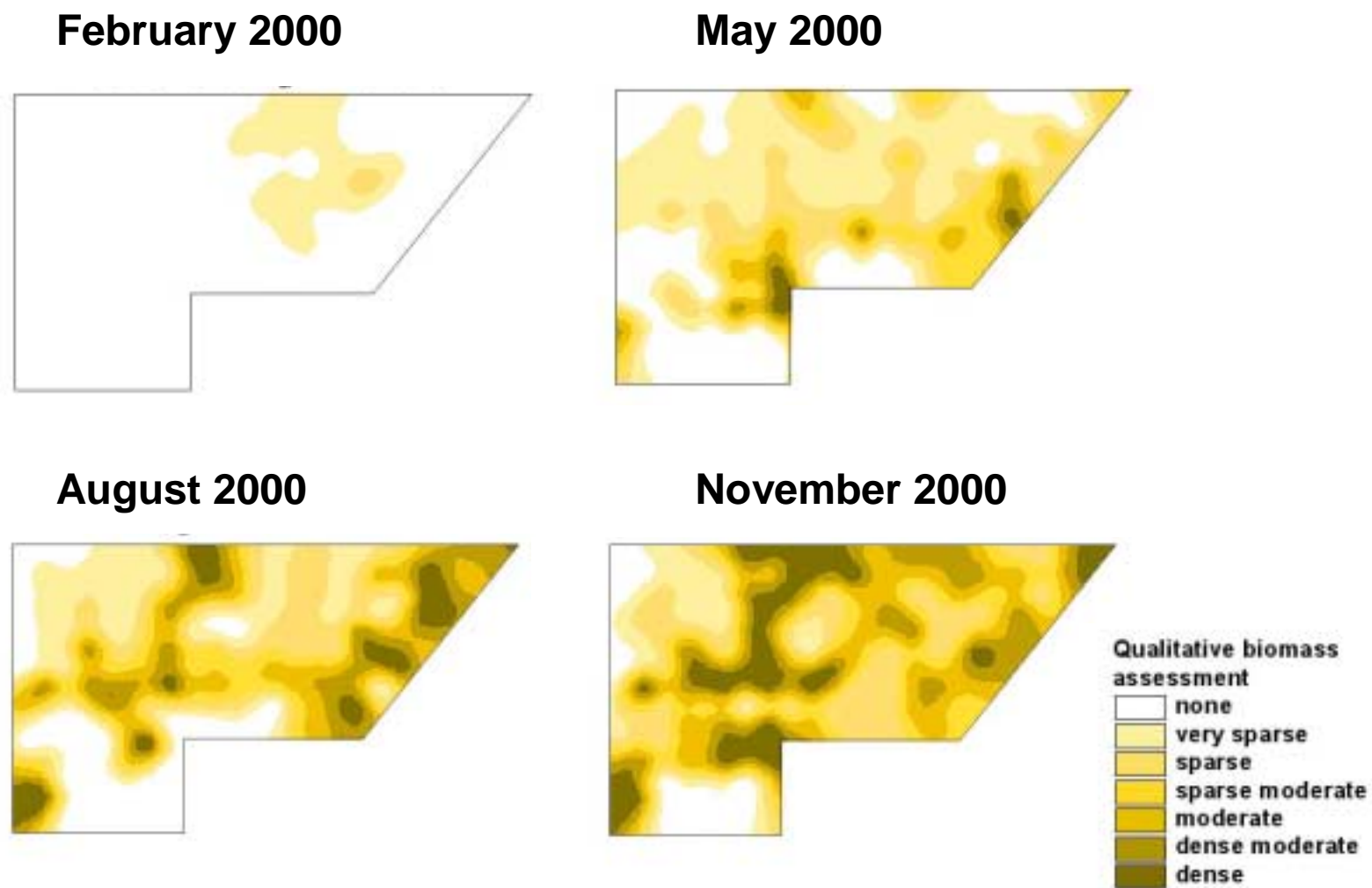


Figure 30. Cell 5 SAV Colonization: Presence and distribution of *Najas* beds during four 120-station visual surveys.

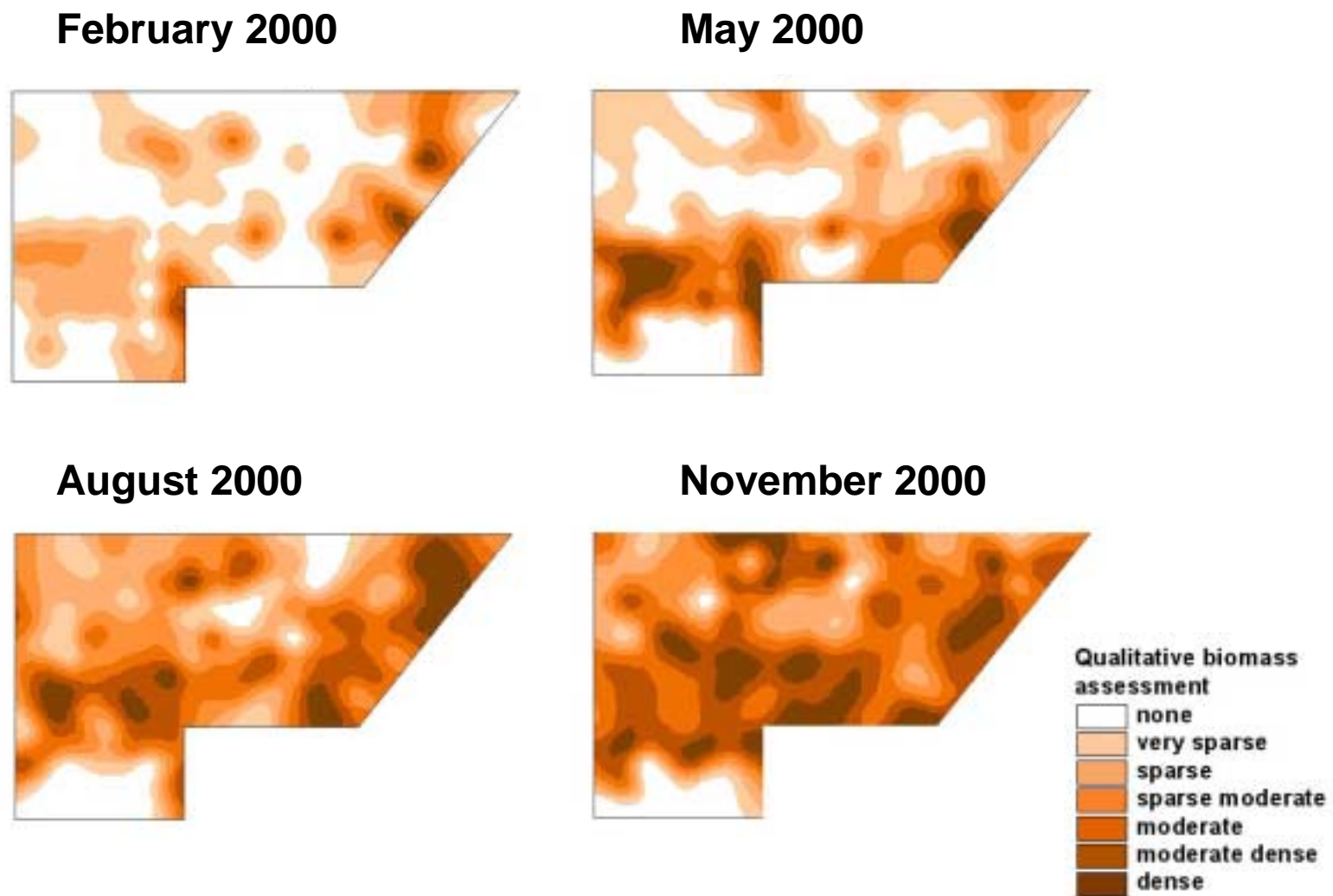


Figure 31. Cell 5 SAV Colonization: Presence and distribution of *Ceratophyllum* beds during four 120-station visual surveys.

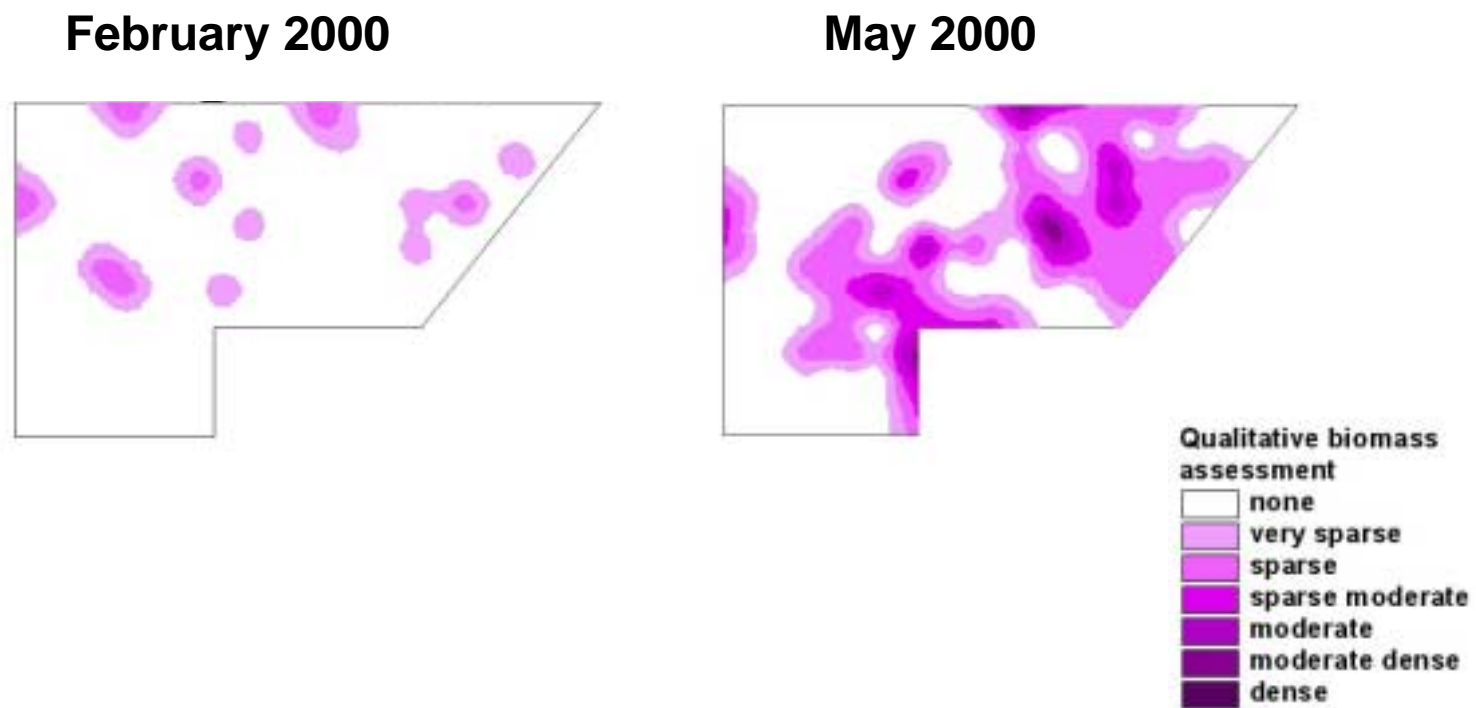


Figure 32. Cell 5 SAV Colonization: Presence and distribution of *Hydrilla* beds during two 120-station visual surveys.

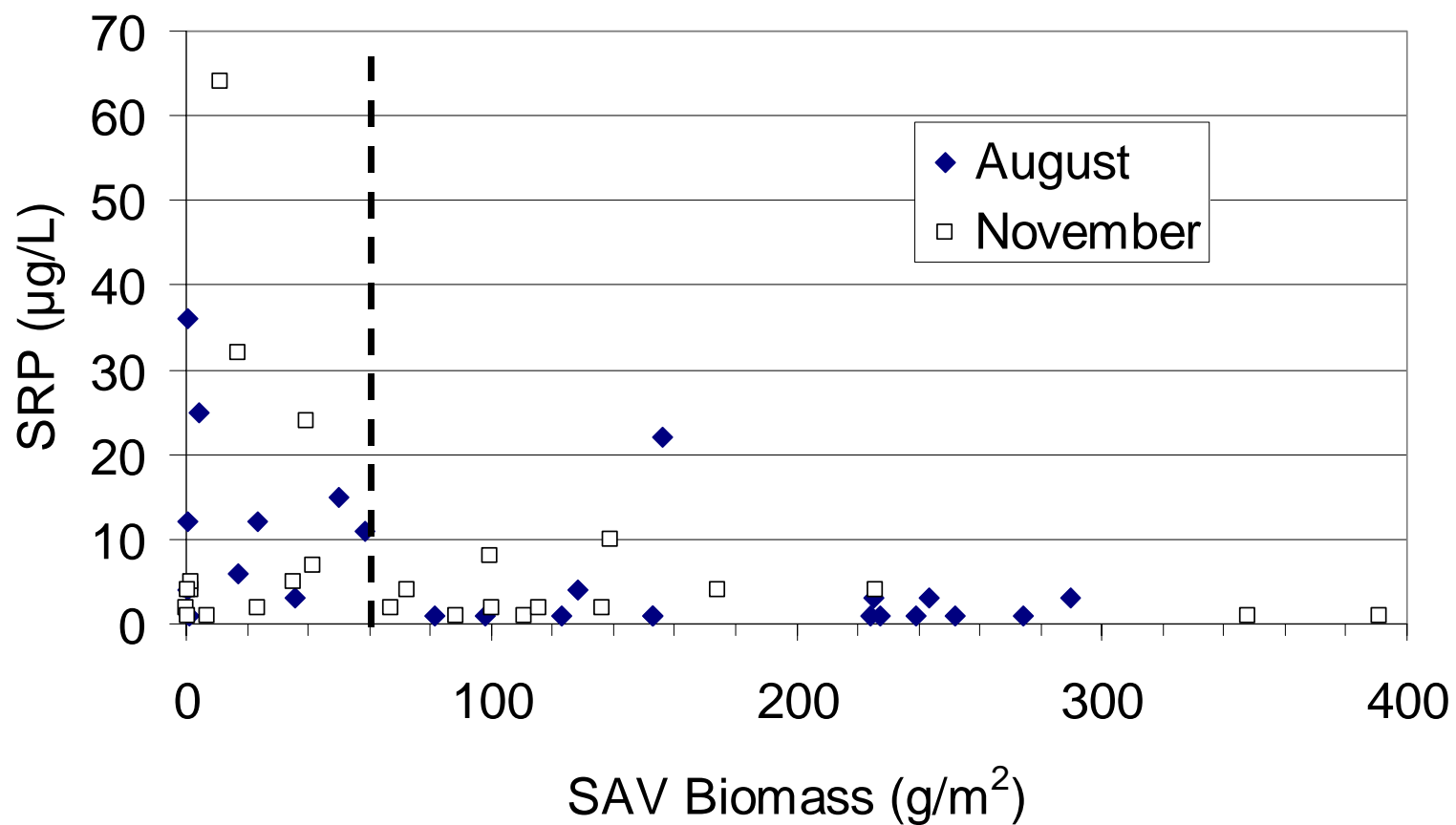


Figure 33. Relationship between SAV biomass and water column SRP concentration at 24 stations internal to Cell 5 on two sampling dates, August 24 and November 30, 2000. The dashed line represents a “threshold” biomass value of 60 g/m². Higher biomass values are associated with SRP concentration of 10 µg/L or less.

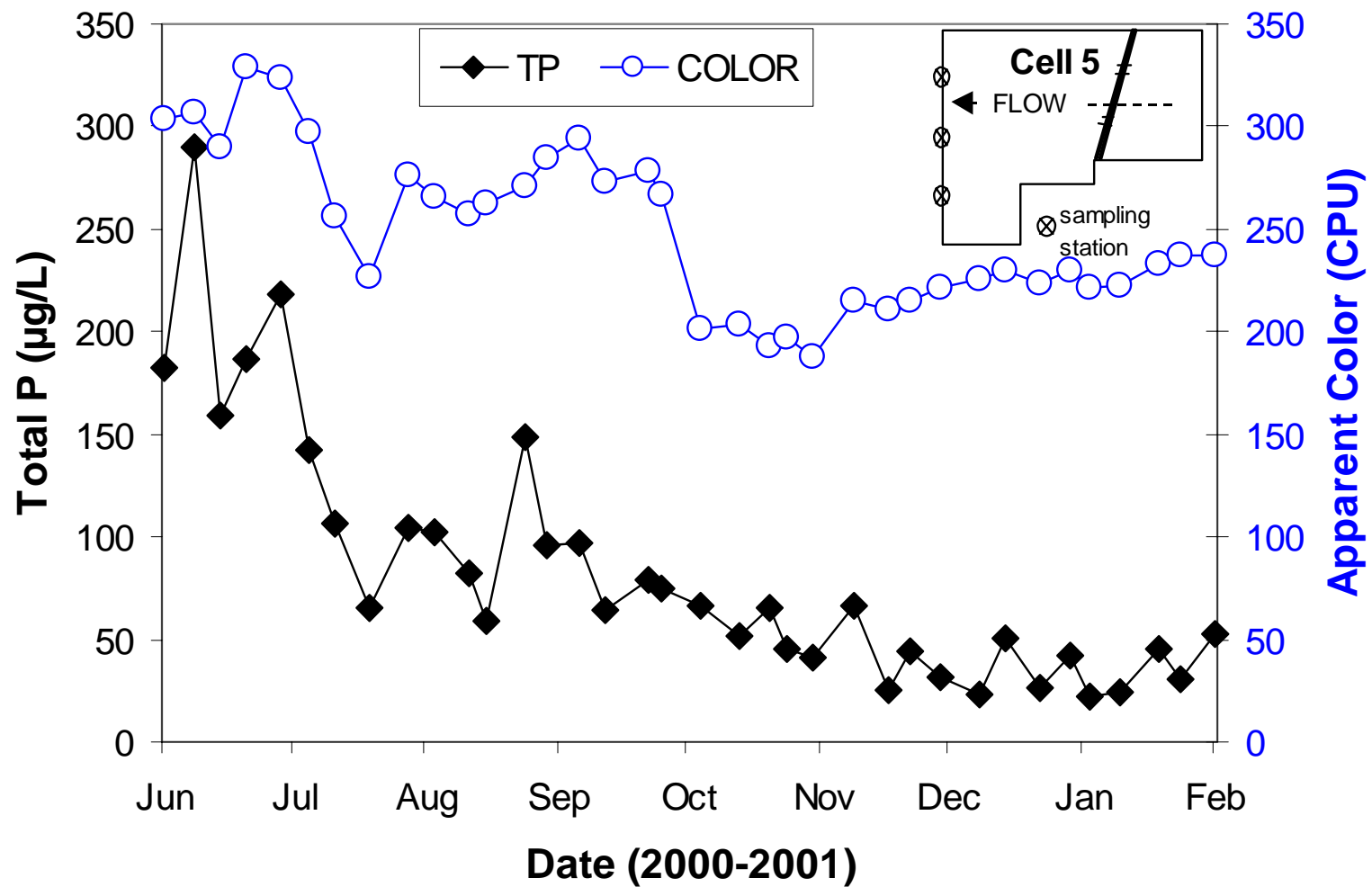


Figure 34. Total phosphorus and apparent color concentrations in the outflow region (inset) of Cell 5.